8-7-2018

Improvement Of Vesicular Stomatitis Virus In Order To Enhance Its Oncolytic Effects

Zahra Enadi
Georgia State University, zibaenadi8@gmail.com

IMPROVEMENT OF VESICULAR STOMATITIS VIRUS IN ORDER TO ENHANCE ITS ONCOLYTIC EFFECTS

by

ZAHRA ENADI

Under the Direction of Professor Ming Luo, PhD

ABSTRACT

Cancer is one of the most deadly diseases around the world. Oncolytic virus (OV) therapy is an anti-cancer approach based on using viruses to selectively target and kill cancerous cells and also their ability to stimulate antitumor immune responses. Vesicular stomatitis virus (VSV) has been investigated as a great platform for an oncolytic agent. Many modifications have been made to VSV to improve its oncolytic effects. One of such modifications by our lab is inserting Smac gene in the genome of VSV to generate armed VSV-S and VSV-Δ55S. The hypothesis is based on the fact that VSV infection triggers apoptosis through the intrinsic mitochondrial pathway, so overexpression of Smac via infection by armed VSV will reinforce apoptosis and increase the rate

of cell killing. We conducted several experiments to examine effects of the inserted gene in viral replication and the enhancement in killing cancer cells compared to wild type VSV.

INDEX WORDS: Oncolytic virotherapy, Vesicular stomatitis virus (VSV), Modification of VSV, Smac gene, Apoptosis, Autophagy

IMPROVEMENT OF VESICULAR STOMATITIS VIRUS IN ORDER TO ENHANCE ITS ONCOLYTIC EFFECTS

by

ZAHRA ENADI

A Thesis Submitted in Partial Fulfillment of the Requirements for the Degree of

Master of Science

in the College of Arts and Sciences

Georgia State University

2018

IMPROVEMENT OF VESICULAR STOMATITIS VIRUS IN ORDER TO ENHANCE ITS ONCOLYTIC EFFECTS

by

ZAHRA ENADI

Committee Chair: Ming Luo

Committee: Donald Hamelberg

Katryn Grant

Electronic Version Approved:

Office of Graduate Studies

College of Arts and Sciences

Georgia State University

July 2018

DEDICATION

I dedicate this thesis to my father who was taken from me far too soon. He has been always source of support and encouragement during every challenge of my life.

This work is also dedicated to my mother who has always loved me unconditionally, stood by me and taught me to work hard for the things that I aspire to achieve.

I also dedicate this thesis to my beloved husband. I am truly thankful for having you in my life. Without his continuous support, love and encouragement it would not have been possible for me to perform this research.

ACKNOWLEDGEMENTS

I am extremely thankful for the opportunity to complete this thesis under the supervision of Dr. Ming Luo. He was one of my best teachers I have ever had in my life. The door of his office was always open whenever I ran into a trouble spot or had a question about my research or writing. His vast knowledge, expertise, guidance and support has provided a solid foundation for me to grow, learn and be successful in completing my research.

I would also like to thank my advisory committee, Dr. Katryn Grant and Dr. Donald Hamelberg for all their support, valuable critique and comments and also their great advice and guidance throughout this project.

I am also thankful to all my lab members who have always been so helpful and supportive and for providing a wonderful collaborative environment to work.

TABLE OF CONTENTS

ACKNOWLEDGEMENTS V

LIST OF TABLES VIII

LIST OF FIGURES IX

LIST OF ABBREVIATIONS X

CHAPTER 1: INTRODUCTION 1

1.1 A brief overview on oncolytic viruses 1

1.2 Mechanism of action by oncolytic viruses 3

1.3 Vesicular stomatitis virus, mechanism of replication 6

1.3.1 Classification of VSV 6

1.3.2 Structure of VSV 7

1.3.3 VSV life cycle 10

1.4 VSV as an oncolytic virus 12

1.5 Modification of VSV 14

1.6 Overall objective and experimental plan 16

2 CHAPTER 2: EXPERIMENT 18

2.1 Cell lines and cell culture 18

2.2 Viruses 18

2.3 Plaque assay 19

2.4 Virus Propagation 20

2.5 Virus purification 20

2.6 Infection of canine oral and anal carcinoma tissues 21

2.7 Western blot 21

2.8 Cell Viability Assay 24

2.9 Autophagy assay 25

3 CHAPTER 3: RESULTS 27

3.1 Comparison of virus growth curves 27

3.2 Virus purification 31

3.3 VSV-S enhanced apoptosis 34

3.4 Assessing autophagy progression 36

3.5 In vitro efficacy of cancer cell killing by VSV-MCP, VSV-S, VSV-Δ55S 39

3.6 ex vivo infection of carcinoma canine oral and anal carcinoma tissues 43

CHAPTER 4: CONCLUSIONS 44

REFERENCES 48

LIST OF TABLES

Table (1). List of potential recombinant vesicular stomatitis viruses created for oncotherapy applications.. 14

Table (2). List of primary and secondary antibodies used for western blotting 23

Table (3). Titer of VSV-MCP and VSV-S at different MOI (HeLa cells) 28

Table (4). Titer of purified VSV-MCP and VSV-S, using HeLa cells 32

Table (5). Percentage of T-47D cell viability infected by VSV-MCP, VSV-S and VSV-Δ55S, at MOI=5, after 24 h post infection 40

Table (6). Percentage of T-47D cell viability infected by VSV-S and VSV-Δ55S, at MOI=5, after 48 h post infection 41

Table (7). Titer of armed viruses and VSV-MCP (MOI=5) at 24 and 48 h post infection, using T-47D cells. 42

LIST OF FIGURES

Figure 1. Mechanism of actions by oncolytic viruses. Adapted from (11)..... 5

Figure 2. VSV virion structure and genome organization. 9

Figure 3. Schematic diagram of VSV life cycle. 12

Figure 4. Schematic diagram of inserted Smac in the viral genome of VSV. 17

Figure 5. Growth curves of VSV-MCP and VSV-S. 31

Figure 6. Titers of purified VSV-S and VSV-MCP. 33

Figure 7. Titers of purified VSV-MCP and VSV-S. 33

Figure 8. Level of Smac (full length and mature) in response to VSV-MCP and VSV-S infection. 35

Figure 9. Evaluating levels of caspase 3 and 9 by western blot. 36

Figure 10. Puncta of LC3. 38

Figure 11. Levels of LC3 I and LC3 II. 39

Figure 12. In vitro efficacy of VSV-S and VSV-Δ55S. 41

Figure 13. Virus titers from T-47D cells infected by different viruses (MOI=5). 42

Figure. 14. ex vivo infection of canine carcinoma tissues with VSV-S and VSV-MCP, respectively. 43

LIST OF ABBREVIATIONS

VSV: Vesicular Stomatitis Virus

VSV-S: Vesicular Stomatitis Virus with full length Smac inserted

VSV-Δ55S: Vesicular Stomatitis Virus with mature Smac inserted

VSV-MCP: Vesicular stomatitis virus expressing mCherry fluorescent protein

Smac: Second mitochondria derived activator of caspase

Caspase: Cystein aspartic proteases

IFN: interferon

TLRs: Toll-like receptors

PKR: protein kinase

OV: Oncolytic Viruses

N: nucleocapsid protein

P: phosphoprotein

M: matrix protein

G: surface glycoprotein

L: large polymerase

GFP: Green fluorescent protein

CHAPTER 1: INTRODUCTION

1.1 A brief overview on oncolytic viruses

Cancer is one of the deadly diseases around the world. It is the result of genetic or epigenetic issues which make changes in normal cells, driving them to become cancerous cells. Malignant cells differ from healthy cells in different aspects; they grow and divide non-stop, which eventually leads to formation of a tumor; tumor cells do not connect to each other, undifferentiated, and have much more variability in cell size and shape; they are able to evade immune system and etc.

There are several ways to treat cancers. The first approach being used more than 4,000 years ago is surgery. The next method was radiotherapy after discovery of X-rays, and another common treatment is chemotherapy (1).

Each of these approaches has their side effects and in many cases patients suffer a lot of pain without being cured. Because of these issues, scientists look for new approaches to overcome these barriers. One of the promising approaches is the use of viruses. The term onco in Latin means cancer and lytic refers to cell destruction or lysis. “Oncolytic viruses” are the ones which applied to destroy cancer cells while having no effects on normal cells.

The discovery of tumor regression by using viruses was in 1912 by observing a patient with cervical carcinoma, showing significant recovery after rabies vaccination for prophylactic treatment after being bitten by a dog (2) . Other reports also showed Burkitt’s and Hodgkin’s lymphomas treatment after infecting with measles virus (3). These phenomena brought much attention to using viruses as an alternative technique instead of common methods for tumor destruction. During 1950s and 1960s, many trials took place and several viruses were tested in vivo and in humans. In one study a vaccine strain of rabies virus was applied in patients with

melanomatosis and the results showed tumor regression for some of them. In the following attempts, the oncolytic efficacy of adenovirus serotype type 4, flavivirus West Nile virus (strain Egypt 101), the paramyxoviruses mumps and Newcastle disease virus (NDV) were tested. There are reports showing use of different kinds of viruses in patients with cervical cancer and other types of advanced cancers. In most cases tumor destruction was not in the way that scientists expected and many side effects also were observed, which causes a halt in these studies (4), (5).

These failures continued about three decades, which may be because of lack of enough knowledge about viral biology, cell cycle control and unsafety of viral treatment. In the late 1980s, advancements in genetic engineering, gene therapy, viral biology, tumor immunology and molecular genetics brought new attentions to oncolytic viruses and many achievements have been made in this area (3).

One of the great advances in the field occurred in 1991, when Martuz et al. reported about a genetically modified herpes simplex virus type I (HSV-1) with a mutation in the thymidine kinase (TK) gene (6). This mutant virus was able to infect and replicate selectively in cancer cells and was efficient in treating brain tumors. This advancement brought attention to improve oncolytic effects of viruses by altering viral genome.

To date, adenoviruses, poxviruses, HSV-1, coxsackieviruses, poliovirus, measles virus, Newcastle disease virus (NDV), reovirus, and others, have entered into early-phase clinical trials. The first genetically modified oncolytic virus approved in China for head and neck cancer in October 2005 was an E1B-deleted adenovirus named Oncorine (H101, the same construct as ONYX-015) (6). The second one approved by the US Food and Drug Administration (FDA) in 2015 was a modified herpes simplex virus type 1 (HSV-1), encoding granulocyte–macrophage colony-stimulating factor (GM-CSF). This virus was named T-Vec (talimogene laherparepvec,

IMLYGIC, formerly OncoVEXGMCSF), and was used for patients with advanced melanoma (6), (7), (8).

The oncolytic viruses have specific characteristics which make them very important in treating malignant cells. First of all, they selectively target cancerous cells, either inherently or by some genetically modifications such as insertion or deletion of genes in their genome or other methods to make them more specific to target tumors. This feature improves the safety of applying these viruses. The second feature is that they will not produce any resistance, since their mechanism of actions includes several pathways for tumor destruction. Another advantage of these viruses is amplification through the course of treatment because of its replication, which is opposed to classical drugs that decrease with time in cancer treatment (9).

Oncolytic viruses can be divided in two major groups. The viruses which are inherently able to infect tumor cells and destroy them without having pathogenic effects in humans. This group includes autonomous parvoviruses, myxoma virus (MYXV; poxvirus), Newcastle disease virus (NDV; paramyxovirus), reovirus, and Seneca valley virus (SVV; picornavirus). The second major group includes genetically modified viruses which have undergone some changes to improve their ability to target cancerous cells, including measles virus (MV; paramyxovirus), poliovirus (PV; picornavirus), vaccinia virus (VV; poxvirus), adenovirus (Ad), herpes simplex virus (HSV), VV, and vesicular stomatitis virus (VSV; rhabdovirus)(9).

1.2 Mechanism of action by oncolytic viruses

The pathways in which oncolytic viruses used to kill cancer cells can be categorized in two major approaches (Fig.1). One will be killing tumor cells directly as the result of viral replication by using cellular transcription and translation mechanisms of host cells (malignant cells). Direct

lysis of infected cells which is the result of cell death happens through different mechanisms of cell death, including apoptosis, autophagy and necrosis. The process of direct cell killing by oncolytic viruses often depends on the type of virus, dosage, the efficiency of targeting a cell receptor, replication of virus, response of cancer cells to viral infection, and the different forms of cell death.

The termination of virus replication cycle results in cell lysis and release of viral particles, tumor-associated antigens (TAAs), cellular damage-associated molecular patterns (DAMPs) like calreticulin, heat shock proteins, high-mobility group protein B1 (HMGB1), pathogen-associated molecular pattern (PAMPs) molecules, cytokines (for example, type I IFNs, tumour necrosis factor-α (TNFα), IFNγ, and interleukin-12 (IL-12)) and cellular ATP in a highly inflammatory process, termed “immunogenic cell death”.

The other major pathway is activation of the host immune system in response to viral and tumor antigens. These antigens activate antigen-presenting cells (APCs) such as dendritic cells that activate natural killer cells and promote activation of antigen-specific CD4+ and CD8+ cytotoxic T lymphocytes. These triggers of the immune system result in destruction of infected and uninfected tumor cells (7), (8) , (9), (10), (11).

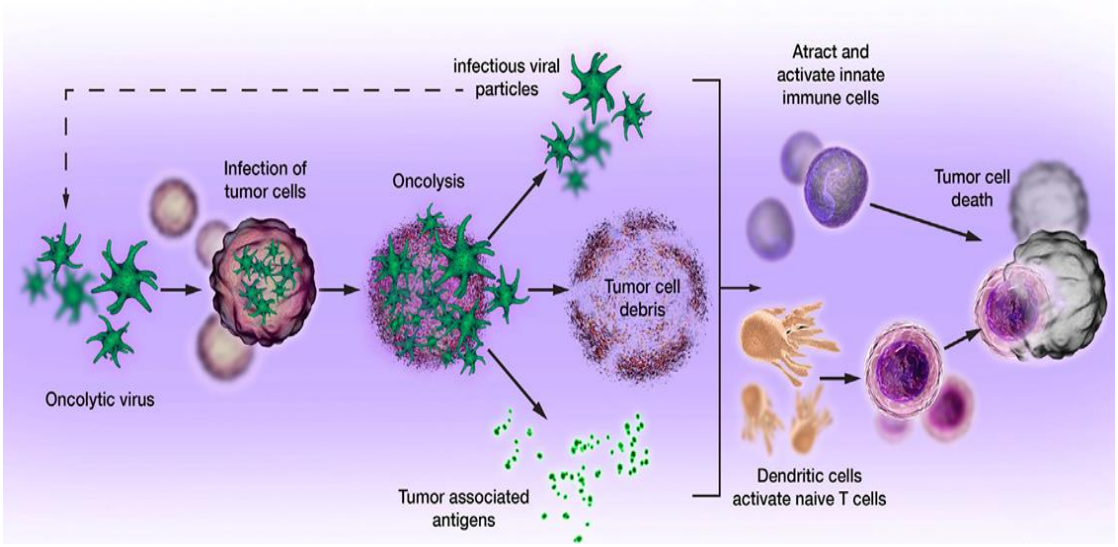

Figure 1. Mechanism of actions by oncolytic viruses. Adapted from (11).

Some viruses are able to selectively infect cancer cells and replicate in them, while others may enter both normal and tumor cells and their replication will be ended in normal cells through antiviral machinery of the host cell. The signaling pathway to eliminate viral replication is complex and may trigger through local interferon (IFN) release or through intracellular Toll-like receptors (TLRs), which are activated by viral elements.

TLRs are receptors which will be activated by recognition of repeated sequences called PAMPs, including viral particles like DNA, RNA and viral proteins. Activation of TLR signaling will induce host immune responses, resulting in termination of viral replication. Another pathway to eliminate virus is through IFN release and following activation of PKR (intracellular protein kinase) which recognizes double-stranded RNA and other viral particles, resulting in termination of cell protein synthesis and eventually cell death and removal of virus (7).

In cancer cells IFN signaling pathway and PKR may be abnormal and because of that, the termination of virus replication will not take place as in normal cells. PKR may be active in some

of cancer cells such as low-grade tumors, causing difficulties in activities of oncolytic viruses and their efficiency (7).

1.3 Vesicular stomatitis virus, mechanism of replication

1.3.1 Classification of VSV

Vesicular stomatitis virus (VSV) is an enveloped virus with a negative sense, nonsegmented, single strand RNA (nnsRNA) which belongs to Rhabdoviridae and is placed in the order Mononegavirales. This virus can infect a wide range of mammals such as horses, cattle, pigs and insects and it causes vesicular lesions in the tongue, oral tissues, udders, and hooves. Vesicular stomatitis is a self-limiting disease and in most cases the infection is not fatal. Infection in humans by VSV is asymptomatic and mild flu like symptoms has been reported after VSV infection. Only accidental cases of human infections have been reported in animal-handlers and laboratory researchers (12-14).

VSV has two different serotypes, Indiana (VSVI) and New Jersy (VSV NJ), which are distinguished by neutralizing antibodies against the G protein. The other difference between these two serotypes is the number and composition of amino acids which showed only 50% identity. The viral proteins also differ in post translational modification and folding. Infection by New Jersey strains is more severe and happens more often than Indiana strains. However, these two stereotypes exhibit similar properties and many studies have been done on VSVI stereotype (13).

VSV has a simple viral genome which encodes five genes, it has a short replication cycle and can infect almost all vertebrate cells and many invertebrate cells. Because of these properties it has been a great model to study basic aspects of virus biology and viral pathogenesis in both in vitro and in vivo systems (14).

1.3.2 Structure of VSV

The mature form of VSV has a bullet shape, and the dimension is approximately 180 nm in length and 80 nm in width. The virion is composed of the host derived plasma membrane, the envelope, and an internal ribonucleoprotein core. The genomic RNA of VSV is very simple and consists of 11, 161 nucleotides. During infection VSV synthesizes five sub-genomic mRNAs that encode its five different proteins: nucleocapsid (N), phosphoprotein (P), matrix (M), surface glycoprotein (G) and large polymerase subunit (L). The five genes and leader and trailer regulatory sequences arranged in the order 3'-(leader), N, P, M, G, L, (trailer)-5',(12, 15). The 47 nt leader and the 59 nt trailer contain sequences functional for transcription, replication and virus assembly. Each gene is flanked by sequences important for generation of capped and polyadenylated mRNAs (Fig.2).

The negative sense, single stranded VSV RNA is enrapped by multiple copies of N protein, forming a helical structure providing a nuclease resistant complex, and is encapsulated in a bullet shaped viral particle (16).

The N protein consists of 422 amino acids, with a net positive charge and always is tightly associated with viral genome inside the virion particle as well as in the infected cells. Crystal structure of N protein bound to RNA revealed that the N protein consists of two separate lobes and the RNA is sequestered inside the grove generated by these two lobes (17). The N protein plays roles in the assembly and regulation of transcription and replication of the N-RNA template (18, 19). The N-RNA complex serves as a template for mRNA synthesis as well as genomic RNA replication.

The N-RNA complex is associated with viral RNA-dependent RNA polymerase (RdRp) which is a complex of the L protein (241 kDa) and the P protein (29 kDa), forming viral

ribonucleoprotein (RNP) complex, responsible for viral transcription and genome replication (20, 21).

The P protein has 265 amino acids and forms a complex with the N protein known as Nº-P complex, before polymerization of N onto the RNA genome (22, 23). The complex is delivered to the replication site by interaction of P with the L protein and the encapsidation happesn by association of N and RNA genome. Since the L polymerase subunit cannot recognize nucleocapsid, P binding is essential for RNA recognition by the L protein and viral replication and transcription. The structure of VSV nucleocapsid in association with the P protein has been solved. It was suggested that th eN protein and the P protein undergo conformational changes upon interaction with the RNA to accommodate the L protein for transcription and replication (17).

The L protein with molecular weight of 250 kDa is essential for viral replication and transcription and functions as a catalytic subunit of the viral polymerase. In addition to RNA synthesis, the L protein also catalyzes mRNA cap addition and cap methylation (24).

VSV has two membrane proteins: the M protein is an internal peripheral membrane protein that is associated with both the nucleocapsid and the lipid bilayer, and the G protein is an integral transmembrane protein that is present on the surface of the virion.(25).

The M protein is one of the most abundant viral proteins and consists of 229 amino acids. The N-terminal region constitutes the signal for membrane binding. The M protein is essential for virus assembly by interacting with the nucleocapsid, the G protein and the cellular plasma membrane, resulting in a bullet shaped structure of virion. The M protein is also important for release of viral particles by budding from the host cells. The M protein plays a crucial role in virus pathogenesis by inhibiting expression of antiviral gene products such as interferon, and proteins

for mRNA export blockage from the nucleus to thwart host innate immune mechanisms. The M protein can activate the intrinsic apoptotic pathway in mammalian cells (26-34).

The G protein is a type I transmembrane protein and is the only protein present in the virus envelope. G proteins exist in the form of trimmers. It is responsible for attachment to the cellular receptor and interactions with the M protein during virus budding. Low pH-dependent conformational changes of the G protein to induce membrane fusion inside the endosome is necessary to release the virion content. VSV particles lacking the G protein are unable to infect cells (25, 34-37).

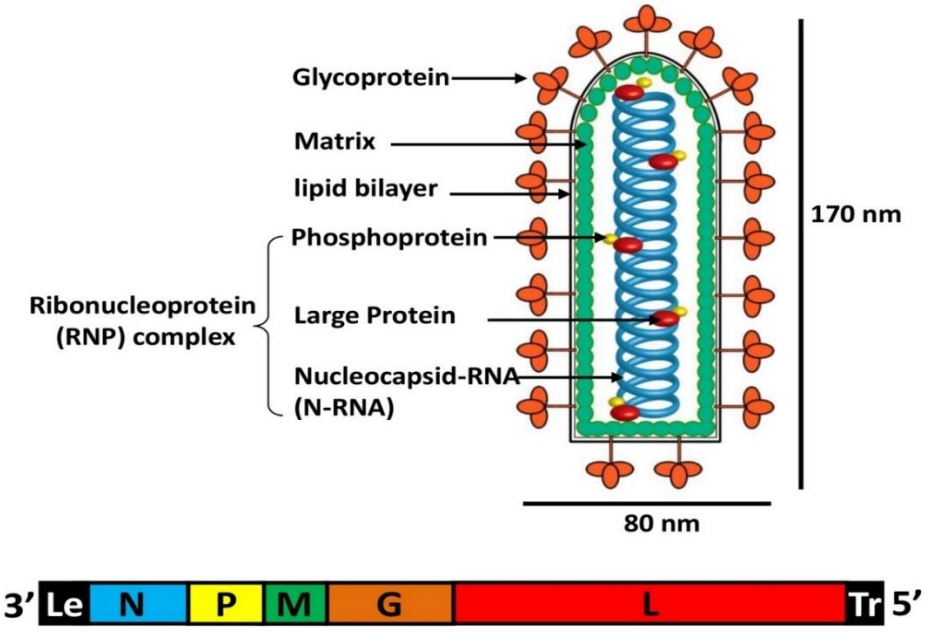

Figure 2. VSV virion structure and genome organization. VSV encodes five structural proteins: nucleocapsid (N), phospho- (P), matrix (M), glyco- (G), and large (L) proteins. The VSV genome is arranged in the order 3'-(leader), N, P, M, G, L, (trailer)-5'. Adapted from(20).

1.3.3 VSV life cycle

VSV replicates entirely in the host cell's cytoplasm. The replication of VSV is initiated after attachment of the G protein to the cell receptor (Fig.3). The host receptor is the LDL receptor and its family members (38, 39). Following attachment, VSV enters host cell through clathrin mediated endocytosis and enters endocytic pathway (40, 41). The pH drops in the endosome (pH below 6.5), leading to a conformational change of the G protein to mediate the fusion of endosomal membrane with the viral membrane and eventually release of ribonucleoprotein (the RNP complex) into cytoplasm where viral replication and transcription take place (42).

During primary transcription, RdRp recognizes specific signals in the N-RNA template and initiates transcription of viral genes directly from the RNA viral genome. The polymerase complex initiates binding at the 3' end of the genome and transcribes 5 mRNAs that are capped and methylated at the 5'end, and polyadenylated at the 3'end in a sequential manner. Each gene is separated by an intergenic region containing signals for poly adenylation and transcriptional start/stop sequences where polymerase complex stutters. There is a probability for RdRp dissociation from the genome at these regions during the polyadenylation, before advancing to transcription of the following gene. Since reinitiation does not always occur, there is a decreasing level of the viral mRNAs (28, 43-45). The abundance of the genes near the 3' end is higher compared to the genes closer to the 5'end, so the N protein has the highest abundance followed by graduate decreasing in the amounts of P, M, G and L mRNAs. Viral proteins will be produced by translation of mRNAs by host ribosome and are required for viral genome replication.

During replication, the polymerase complex ignores all of the initiation, termination, and polyadenylation signals utilized to produce mRNAs, and synthesizes a complementary full-length

anti-genome. Replication of the genomes requires N and P proteins, and it has been proposed that the P protein keeps the N protein in a soluble encapsidation competent form (22, 46).

The anti-genome will then act as a template and the polymerase complex will replicate the full-length VSV genome. These newly synthesized genomes can be used as a template for secondary transcription or assembled into new virions (33, 47).

M and G proteins play an essential role in the assembly and budding which take place at the plasma membrane (48, 49). The G protein is glycosylated in the ER and transported to the Golgi apparatus where the complete glycan moieties are added, and then through cellular secretory pathway is transported to the plasma membrane, forming membrane microdomains which is important for VSV budding (50). M proteins are also transferred to the plasma membrane where they form microdomains in association with the plasma membrane independent of the G protein (25, 51). In cytoplasm the viral genome is encapsidated by the N protein and assembled with the polymerase complex (P and L proteins), then transported to the plasma membrane in a microtubule dependent manner to become associated with M protein (52, 53). This complex is assembled into mature VSV virions. The M protein recruits cellular proteins at the site of budding for final release of mature infectious virions, (53-55).

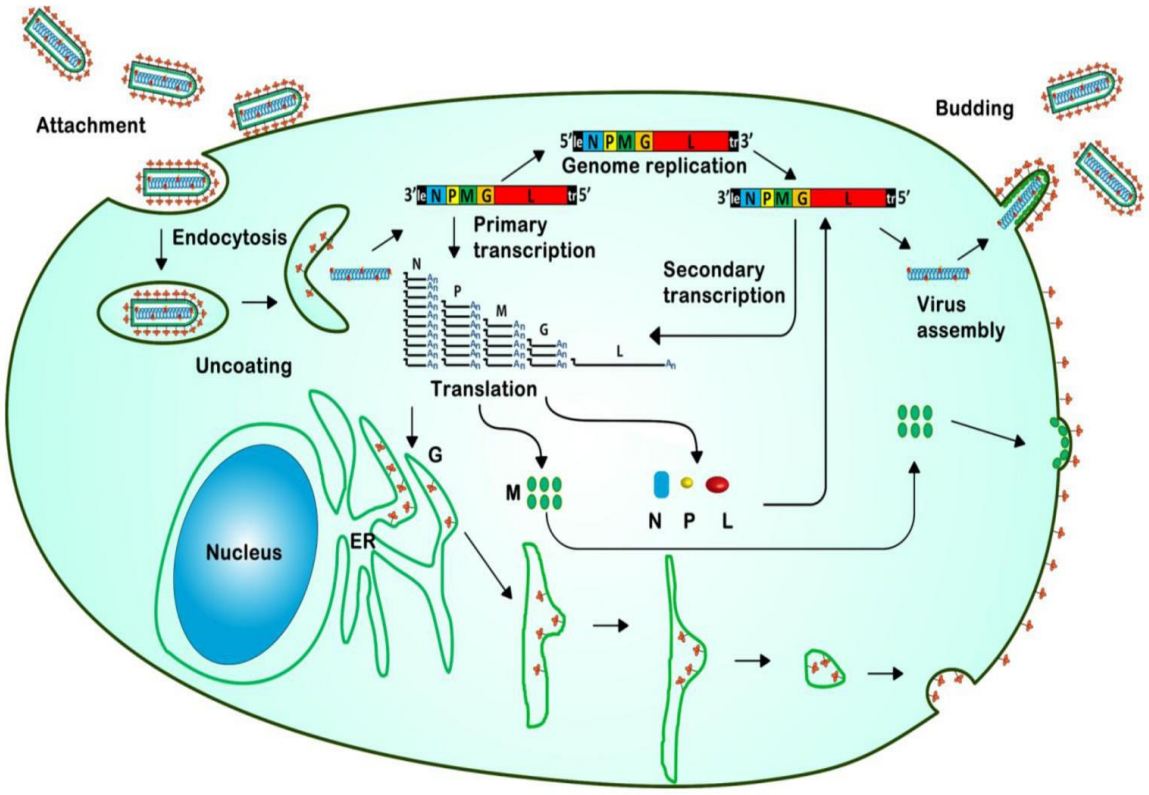

Figure 3. Schematic diagram of VSV life cycle. Steps of virus life cycle: attachment, endocytosis, uncoating, genome replication, mRNA transcription, viral protein translation, viral assembly, and budding are shown. Adapted from (15).

1.4 VSV as an oncolytic virus

VSV is a natural oncolytic virus which preferably targets and replicates in various types of cancer cells, in vitro and in vivo (12, 56-58). Immune signaling pathways in malignant cells are generally defective, which is important for proliferation and evasion from tumor suppression mechanisms of host immunosurveillance (59, 60).

It has been shown that the effectiveness of VSV to replicate in immortalized and malignant cells is mainly due to a defective of type I interferons (IFNs) pathway or PKR function (12, 61). The interferons are a family of cytokines produced in response to viral infection and play essential

roles in antiviral innate immunity response (32, 62). Defectiveness in PKR that mediates the innate immune signaling pathway will cause the inability of cancer cells to suppress translation of viral proteins (63, 64).

In addition, tumors with mutations in the tumor suppressor p53, or activated Myc- or Ras-signaling cellular aberrations that occur in over 90% of all tumors, were reported to be susceptible to VSV-mediated oncolysis (57, 65).

Replication of VSV in healthy cells with normal and effective antiviral immune response will be suppressed because of both the innate and adaptive immune response (66, 67). In normal cells, activation of the innate immune system following infection by VSV results in production of beta interferon (IFN-β) which activates IFN stimulated genes to upregulate the antigen processing machinery and activate antigen cells such as dendritic cells, NK cells and macrophages (68, 69). Activation of the IFN signaling pathway results in viral gene expression suppression and infected cell clearance via leukocytes (16, 69, 70).

Using VSV as an oncolytic vector has many advantages, making it a good platform for onco virotherapy. First of all it has a short replication cycle which allows it to reach a high titer in a short time of infection, resulting in faster spread of virus in the tumor and a fast lytic cycle (14). Secondly, VSV will not cause any host-cell transformation nor any immune-mediated pathogenesis. Thirdly, VSV has been studied for many years and its well-studied biology makes it possible to manipulate the simple genome of VSV via reverse genetics to enhance its oncoselectivity, safety, oncotoxicity and stimulation of tumour-specific immunity. Beside these, the viral envelope glycoprotein (G) targets a large variety of cancer cells because of its ubiquitous receptor mechanism, and the G protein has been modified to establish several pseudotype viruses (71, 72). VSV is not a human pathogen likely because of the induction of strong immune responses

to suppress viral replication and amplification so there is not any preexisting immunity in humans that could limit clinical applications (73-75). VSV is not gene attenuated, which affects replication and therefore oncolytic antitumor activity (76).

1.5 Modification of VSV

Many modifications have been made to VSV to generate recombinant VSVs (rVSV) to improve tumor targeting, safety, oncotoxicity, reduction of premature immune clearance, inducing controlled apoptosis and triggering anti-tumor immune response (14, 58). The improvements in reverse genetic made it possible to manipulate the genome of VSV and generating novel VSV vectors expressing genes of interest.

There are different approaches to enhance the oncolytic effects of VSV, including combination of VSV with chemical agents, insertion of tumor suppressor genes in viral genome, combining VSV with anti-angiogenic agents, radiovirotherapy, creating rVSVs expressing pro-apoptotic, immunomodulatory, or suicide cassettes, micro RNA targeting, stimulating interferon induction, expression of cytokines or immune-stimulatory molecules (14, 77).

Some of recombinant VSVs which have been engineered for oncotherapy are summarized in Table (1).

Table (1). List of potential recombinant vesicular stomatitis viruses created for oncotherapy applications. Adapted from (14).

VSV modification	Virus description
VSV-IL4	rVSV expressing IL-4 cytokine with enhanced oncolytic activity
VSV-IFN	rVSV expressing IFN- gene, show oncolytic activity against metastatic lung disease, and able to generate T cell response

VSV-IL12	rVSV is expressing murine IL-12 gene show oncolytic activity against squamous cell carcinoma.
rVSV- gG	rVSV expressing equine herpes virus-1 glycoprotein G, which acts as a broad-spectrum viral chemokine binding protein
rVSV-UL141	rVSV expressing a protein from human cytomegalovirus which down regulates the natural killer (NK) cell-activating ligand CD155 and inhibits the function of NK cell
rVSV(MD51)-M3	rVSV expressing the murine gammaherpesvirus-68 chemokine-binding protein M3 in modified matrix protein backbone with enhanced tumor necrosis
DM51-VSV	DM51-VSV infection activated DCs to produce proinflammatory cytokines (IL-12 and IFNs)
VSV-CD40L	rVSV expressing CD40L, a member of the TNF family expressed on the surface of activated Th cells
VSV-p14	rVSV expressing p14 FAST protein increase oncolytic property
VSV-CD133	rVSV expressing CD133 (a marker for cancer stem cells) increase specificity for CD133 expressing tumours.
VSV-IL15	rVSV expressing secreted version of human interleukin15, it enhances both NK cell and T cell response
VSV-mp53 and VSV-DM-mp53	VSV-mp53 and VSV-DM-mp53 both expressing high level of functional p53 in respective backbone VSV with chemical compounds
VSV-TK	rVSV expressing thymidine kinase of herpes virus, increase oncolytic property

LCL161 and VSV-DM51	SMC and OV therapies combination also synergize in vivo by promoting anticancer immunity through an increase in CD8+ T-cell response

TNF: tumor necrosis factor; DC: dendritic cells; NIS: sodium iodide symporter; SMC: Second mitochondrial activator of caspase (Smac)-mimetic compounds.

1.6 Overall objective and experimental plan

The ultimate goal of oncolytic virotherapy is selectively killing cancerous cells. As explained in previous section many modifications of VSV have been carried out to achieve this goal. The aim of this study is to enhance oncolytic effects of VSV by engineering new armed VSV via inserting Smac gene (full length or mature form) in the viral genome between the M and G genes (Fig.4). The hypothesis is based on the fact that VSV infection induces apoptosis through the intrinsic mitochondrial pathway (32, 78). Previous studies also showed that autophagy plays a cytoprotective role and supports virus replication in VSV and some other virus infections, and inhibition of autophagy will trigger apoptosis (79). Our optimal design will be induction of apoptosis after having an adequate amount of virus production, which will be achieved by properly expression of Smac with armed VSV-S (full length Smac inserted) and VSV- Δ55S (mature form inserted).

Smac (Second mitochondria-derived activator of caspase), also known as DIABLO (Direct Inhibitor of Apoptosis-Binding protein with LOw pI), is a mitochondrial protein. Upon presence of apoptosis stimuli, the mature form of Smac, which is generated by cleavage of the mitochondrial targeting signal from N-terminal domain of full length Smac, is released to the cytosol. Mature form of Smac will interact with IAPs (inhibitor of apoptosis proteins) and prevent their association with caspase 9 and therefore promote activation of caspase 3 and apoptosis (80, 81).

We conducted several experiments to examine the effect of inserted Smac in viral replication by using several cell lines and also evaluate the efficacy of armed VSV-S and VSV-Δ55S in killing cancerous cells compared to wild type VSV.

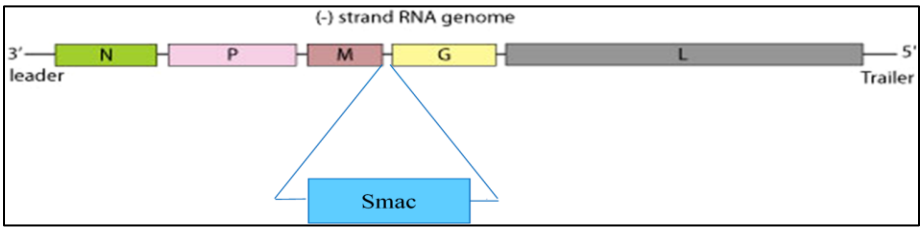

Figure 4. Schematic diagram of inserted Smac in the viral genome of VSV.

2 CHAPTER 2: EXPERIMENT

2.1 Cell lines and cell culture

HeLa, Vero, and T-47D cell lines were from ATCC (American Type Culture Collection, Manassas, VA, USA). HeLa expressing GFPLC3 (HeLa GFP-LC3) cell line was a gift from Dr. Wen-Xing Ding at the University of Kansas Medical Center, USA. Anal and oral carcinoma canine tissues was kindly provided by Dr. Nicole Northrup, Associate Professor of Oncology at University of Georgia (UGA).

HeLa, Vero and HeLa GFP-LC3 were cultured in Dulbecco's Modified Eagle Medium (DMEM, Gibco, Life Technologies Corporation, UK) supplemented with 10% fetal bovine serum (FBS, American Type Culture Collection, Manassas, VA, USA) and 1% penicillin/streptomycin (Gibco, Life Technologies Corporation, USA) at 37 °C, 5% CO2, in a humidified incubator. T-47D cells were propagated in RPMI 1640 (American Type Culture Collection, Manassas, VA, USA) supplemented with 10% FBS, 1% penicillin/streptomycin and human insulin at 37 °C, 5% CO2, in a humidified incubator. Anal and oral carcinoma canine tissues were maintained in DMEM containing 1% penicillin/streptomycin at 37 °C, 5% CO2, in a humidified incubator.

2.2 Viruses

Vesicular stomatitis virus expressing mCherry fluorescent protein (VSV-MCP), vesicular stomatitis virus with full length Smac gene (Second mitochondrial-derived activator of caspase) inserted between the M and G genes of VSV genome (VSV-S) and vesicular stomatitis virus with the mature form of Smac (55 N-terminus amino acids removed) inserted (VSV-Δ55S) were from Dr. Ming Luo.

2.3 Plaque assay

The plaque assay, a well-known and accurate method for quantification of virion particles, was used to measure the titer of viruses as plaque-forming units per ml (PFU/ml). The principle of this assay is based on the infection of monolayer cells with different dilutions of the virus under study (unknown concentration). Cells are washed with warm Dulbecco's phosphate-buffered saline (DPBS) (Gibco, Life Technologies Corporation, USA) and the virus inoculum is added. After one-hour virus absorption, infected cells are washed with DPBS again and are covered with an agarose overlay to limit spread of the virus. The virus replicates within infected cells, which eventually makes cells become lysed. The adjacent cells will become infected and after several infection cycles, they will be lysed. The plaque refers to each group of lysed cells surrounded by uninfected cells and is assumed as one original single virus. Staining monolayer cells with crystal violet makes it easier to count plaques and by applying in the following formula, the titer of virus can be measured.

$$PFU/ml = \frac{Average\ number\ of\ plaques}{(Dilution\ factor) \times (volume\ of\ diluted\ virus)}$$

For this experiment, HeLa cells were grown in 12-well plates to the confluency around 90% and after washing with DPBS, serial dilutions of viruses (VSV-MCP, VSV-S and VSV-Δ55S) were added to different wells. The plate was incubated at 37 ºC, 5% CO_2, in a humidified incubator for 1 h and meanwhile was rotated every 10 minutes. The cells were then washed with DPBS. For overlay, 0.8% of agarose (SeaPlaque Agarose, Lonza) dissolved in DMEM without FBS was made and about 700 µl was added to each well. The plate was placed in room temperature for about 10 minutes to let the overlay become solid. The plates were subsequently incubated for 24 to 48 h and monitored routinely to check the plaque formation. For fixing the cells, formaldehyde (Formalin solution, neutral buffered, 10%, Sigma) was added to each well and kept in room temperature for

30 minutes. Before staining, formaldehyde and agarose overlay were rinsed off with water and cells were covered with small amount of 0.1% crystal violet solution (Crystal Violet, 1% stain, Fisher Science Education) and stained for 5 to 15 minutes. The crystal violet solution was washed off gently with water and the plaques were counted for each virus.

2.4 Virus Propagation

HeLa or Vero cells were seeded on 150 mm plates using DMEM supplemented by 10% FBS and 1% penicillin/streptomycin and incubated at 37°C, 5% CO_2, in a humidified incubator until reaching the confluency of 80-90%. After removing the media, cells were washed with DPBS and the inoculum of VSV-MCP, VSV-S or VSV-Δ55S at MOI=0.1 was added. MOI refers to multiplicity of infection, defined as

$$\text{MOI}= \frac{PFU\ of\ virus}{number\ of\ cells}$$

The plates were incubated for one hour, meanwhile rotated every 10 minutes to allow virus adsorption. After virus absorption, 12 ml of fresh DMEM without FBS was added to each plate, and the plates were incubated for 48 h. Based on the rate of virus replication, the incubation time may differ for each cell line or virus.

2.5 Virus purification

The supernatant from plates infected by different viruses was collected and centrifuged at 9,500 rpm for 15 minutes at 22 °C for clarification. The clarified virus-containing supernatants were collected in new clean tubes and were centrifuged at 16,100 rpm for 2 hours, at 4 °C. The pellets were resuspended in phosphate-buffered saline (PBS) (Gibco, Life Technologies

Corporation, USA) with 5% sucrose, and the titers were determined by plaque assay. The purified viruses were stored at -20 °C for further usage.

2.6 Infection of canine oral and anal carcinoma tissues

The tissues were deposited in DMEM supplemented by 10% FBS and 1% penicillin/streptomycin. In the cell culture hood, using a sterilized biopsy core and forceps, different cores from various regions of tissues were collected and each core was divided evenly in two halves with a sterilized razor blade. In different wells in a 12-well plate, tissues were deposited and washed three times by DPBS. 1×10^5 PFU of VSV-S and VSV-MCP were used to infect the tissues, and at different time point of post infection (24, 48 and 72 h) the supernatant was collected to determine the virus titer by plaque assay.

2.7 Western blot

HeLa cells were grown in 60 mm plates using DMEM supplemented with 10% FBS and 1% penicillin/streptomycin. For western blot, cells were washed with ice-cold PBS and were lysed by adding 1 ml RIPA Lysis Buffer (0.5 M Tris-HCl, pH 7.4, 1.5 M NaCl, 2.5% deoxycholic acid, 10% NP-40, 10 mM EDTA, 10X, Millipore). By aid of a cell scrapper, adherent cells were detached and cell suspensions were transferred to a new clean Eppendorf tube. The tubes were centrifugated for 1 to 5 minutes at 13,000 rpm using a micro centrifuge, and supernatants from each tube were transferred to new tubes. The lysates were mixed with the equal volume of Laemmli buffer (4% sodium dodecyl sulfate (SDS), 10% 2-mercaptoethanol, 20% glycerol, 0.004% bromophenol blue, 0.125 M Tris-HCl, the pH adjusted to 6.8), and then boiled for 5 minutes at 100 °C, followed by spin down for 1 minute.

Samples and a protein ladder (GeneRuler, #SM1811/2) were loaded in a 15% SDS-PAGE gel, and then the cassette holding the gel was placed in a tray containing the running buffer (25 mM Tris base, 190 mM glycine, 0.1% SDS, the pH adjusted to 8.3). The electrophoresis was carried out at a constant 100 v for 1-2 hour.

After gel electrophoresis the proteins from the gel were transferred to the nitrocellulose membrane using a Bio-Rad Mini Trans-Blot SD Semi-Dry Electrophoretic Transfer Cell apparatus (Mini Trans-Blot® Cell and Criterion™ Blotter). In the transfer process, voltage was applied to transfer the proteins from the gel to the membrane. First, the membrane was cut to the dimension of the gel and was soaked in transfer buffer (25 mM Tris Base Saline (TBS), 192 mM Glycine, 20% Methanol, pH: 8.3) to make it completely wet. The membrane was placed between the gel and the positive electrode in a sandwich. The sandwich was setup by placing sponges at each end, filter papers to protect the gel and blotting membrane, and the gel and the membrane. The sandwich was held with a gel cassette holder and placed in the buffer tank that was filled with transfer buffer. The negatively charged proteins were transferred to the membrane from the gel by applying voltage that generated 120 milliampere for around 2 hours.

The next step was blocking the membrane with 2% BSA (bovine serum albumin) dissolved in 1% TBST (Tris buffered saline-Tween 20) at 4°C for 2 hours for preventing antibodies from binding to the membrane nonspecifically. The membrane was washed three times by TBST 1% and incubated with the desired dilution of primary antibodies overnight at 4°C. The membranes were washed three times with TBST 1%, 5 minutes for each wash and incubated with the secondary antibody at room temperature for 1 hour. The washing step was repeated. For visualizing the bands, the membrane was incubated with Horseradish peroxidase substrate (Luminata Forte, Western HRP Substrate) in a dark place for 5 to 10 minutes. After removing the

excess reagent, the membrane was covered in a transparent plastic bag and a film was put on top inside a film cassette. The images were developed using a film developer machine (X-OMAT 2000A, Kodak). Protein molecular weights were estimated by comparing visible bands from each sample to bands generated from the protein ladder.

Table (2). List of primary and secondary antibodies used for western blotting

Antibody	Dilution	Type	Company
β-actin	1:1000	Rabbit polyclonal	Abcam company (#ab8227)
GAPDH	1:1000	Rabbit polyclonal	Abcam company (#ab9485)
Smac	1:500 or 1:1000	Rabbit Monoclonal	Epitomics (#1012-1)
Cleaved Caspase-3	1:500 or 1:1000	Rabbit Ab	Cell Signaling Technology (#9661)
Caspase-9	1:500 or 1:1000	Rabbit Ab	Cell Signaling Technology (#9502)
LC3 A/B	1:500 or 1:1000	Rabbit Ab	Cell Signaling Technology (#4108)
Secondary Anti-Rabbit	1:1000	Polyclonal, Goat anti-Rabbit IgG	Thermo Fisher Scientific (# 31460)

Secondary Anti-Mouse	1:10000	Polyclonal, Goat anti-Mouse IgG	Thermo Fisher Scientific (# 31430)

GAPDH and β-actin were used as a loading control and all antibodies were diluted in 2% BSA dissolved in 1% TBST.

2.8 Cell Viability Assay

The MTT assay, a sensitive, quantitative and colorimetric experiment, was used to determine cell viability. MTT, a yellow tetrazolium salt, stands for 3-(4,5-dimethylthiazol-2-yl)-2,5-diphenyltetrazolium bromide. It may be reduced by viable cells containing NAD(P)H-dependent oxidoreductase enzymes to formazan, an insoluble crystalline product with a deep purple color.

Formazan crystals are then dissolved using a solubilizing solution (stop solution) and absorbance is measured at 500-600 nanometers using a plate-reader. The darker the solution, the greater the number of viable, metabolically active cells will be.

For calculating the percentage of viable cells, the absorbance reading of the blank (or background, the ones treated by 1% Triton) was subtracted from all samples. Absorbance readings from test samples was divided by those of the control and multiplied by 100 to give the percentage of cell viability.

$$\%\ viable\ cells = \frac{abs\ sample - abs\ background}{abs\ control - abs\ background} \times 100$$

For this experiment, T-47D cells were seeded in 12-well plates, and maintained in RPMI 1640 supplemented with 10% FBS, human insulin and 1% penicillin/streptomycin. After reaching to around 80% confluency, cells were washed with DPBS and infected with VSV-MCP, VSV-S and VSV-Δ55S, respectively, at MOI=5. Supernatants were collected at 24 and 48 h to examine titer

of viruses. The uninfected cells were used for control and background absorbance. For wells of background absorbance, 1% Triton X-100 (dissolve in PBS) was added to kill cells. Cells viability were measured after 24 and 48 h post infection. After removing the media, 200 µl of warm PBS and 30 µl of MTT dye (CellTiter 96®, Promega Corporation, and USA) were added to each well. Plates were incubated at 37 °C, in a humidified incubator for about 2 hours until the purple color has appeared. The reaction was stopped by adding 200 µl of stop solution (Solubilization solution/Stop Mix, Promega Corporation, USA) and plates were incubated at room temperature while shaking for 5 hours. MTT dye is sensitive to light so that the steps after adding dye were performed in a dark place and plates were covered. The final step was reading the absorbance at 570 nm using a plate reader and the percentage of cell viability was calculated according to the given formula.

2.9 Autophagy assay

Microtubule-associated protein light chain 3 (LC3), involved in the formation of autophagosomes and autolysosomes, is a marker to evaluate autophagy. One reliable and quantitativ assay to evaluate autophagy is to monitor, characterize and measure the number of GFP-LC3 puncta (Green fluorescent protein diffused at the amino terminus of LC3) by fluorescence microscopy (82). For this method, HeLa cell line expressing GFP-LC3 was grown in DMEM supplemented with 10% FBS and 1% penicillin/streptomycin. Coverslips were sterilized, following protocol for Glass Coverslip Cleaning (Light microscopy core facility, Duke University). Base on the protocol, glass coverslips were cleaned by using HCl (1M) at 50-60 ºC and occasional agitation for 4 to 16 hours. They were then washed with distilled water to remove acid, followed by rinsing with ethanol (100%). After washing, the coverslips were dried using

paper tissues and kept in a clean container under laminar hood. For cell culture, sterilized coverslips were placed at the bottom of each well in 6-well plates and 1 ml of cell suspension was dispensed in each well.

The plates were checked routinely to make sure that cells were attached to coverslips and were growing well. Before imaging, old medium was aspirated, and cells were washed with PBS and fixed with 1 ml formaldehyde (Formalin solution, neutral buffered, 10%, Sigma) for 15 min at 37 °C in a humidified incubator. Afterwards, formaldehyde was aspirated and coverslips were rinsed with PBS, and the remaining PBS was gently removed by putting them on the tissue. The final step was adding one drop of slide oil on a glass slide and the coverslip was mounted on the slide, in the orientation that the cells on the coverslip faced the oil. Slides were labeled properly and observed under a fluorescent microscope. A number of images was taken from each coverslip and the average number of GFP-LC3 puncta was determined from a number of cells.

3 CHAPTER 3: RESULTS

3.1 Comparison of virus growth curves

VSV is a good platform as an oncolytic virus and many modifications have been done to enhance its tumor targeting, safety and oncotoxicity in order to overcome premature immune clearance and/or to induce or stimulate anti-tumor immune responses (58). VSV is a potent inducer of cell death due to the activation of multiple apoptotic pathways (78, 83-86). Some studies also showed that overexpression of Smac/DIABLO sensitized tumors to chemotherapeutic drugs, or combination of oncolytic viruses with Smac could eradicate tumors (80, 81, 87, 88). Based on all previous studies, we hypothesized that modification of VSV genome by inserting Smac gene (full length and mature form) as an expression unit between M and G genes will promote more robust oncolysis by this armed VSV. The first thing to examine about armed VSV-S was to evaluate the impact of inserted Smac gene on viral replication. For this study virus growth curves were determined to evaluate replication of armed viruses compared to VSV-MCP as a control.

Study of virus growth curves was carried out by using HeLa cells as described below.

HeLa cells was grown to the confluency of 3.2×10^6 cells per 60 mm plate and were infected with VSV-MCP and VSV-S, respectively, at different MOIs (MOI= 1, 0.1, 0.01). The volume of viruses needed for each MOI was calculated and fresh DMEM without FBS was added to the final volume of 1 ml. The plates were kept at 37 °C, 5% CO_2, in a humidified incubator for one hour and meanwhile were rotated every 10 minutes to allow virus adsorption and penetration evenly in the plates. After that, the plates were washed with DPBS and 3 m of DMEM without FBS added to each plate and were kept in the incubator. Samples from supernatant were taken at different time points (4, 8, 12, 24 and 36 h of post infection). The aliquots were stored at -20°C

until all samples were collected and their titers were determined by plaque assays in triplicate. Virus growth curves were plotted based on the average of virus titers at different MOI versus time point post infection. Our results (Table (3), Fig. 5) indicate that VSV-S grew at the same or higher rate as VSV-MCP, suggesting that insertion and expression of Smac does not comprise VSV replication.

Table (3). Titer of VSV-MCP and VSV-S at different MOI (HeLa cells)

Virus	**POST INFECTION (h)**	**MOI=1**		**MOI=0.1**		**MOI=0.01**	
		# of plaques	**PFU/ml (log 10)**	**# of plaques**	**PFU/ml (log 10)**	**# of plaques**	**PFU/ml (log 10)**
VSV-S	36 h (10^{-6})	6	7.48	12	7.78	18	7.95
		9	7.65	9	7.65	19	7.97
		7	7.54	8	7.6	11	7.74
	STDEV		0.08621678		0.092916		0.12741
	Average		7.55		7.67		7.88
VSV-MCP	36 h (10^{-6})	1	6.69	5	7.4	11	7.74
		3	7.18	7	7.54	8	7.6
		9	7.65	8	7.6	10	7.7
	STDEV		0.48003472		0.102632		0.072111
	Average		7.17		7.51		7.68
	24 h (10^{-5})	13	6.81	54	7.43	51	7.41
		19	6.97	43	7.33	32	7.2
		33	7.21	65	7.51	38	7.28
	STDEV		0.20132892		0.090185		0.105987
	Average		6.99		7.42		7.29

Virus	POST INFECTION (h)	MOI=1		MOI=0.1		MOI=0.01	
		# of plaques	PFU/ml (log 10)	# of plaques	PFU/ml (log 10)	# of plaques	PFU/ml (log 10)
VSV-MCP	24 h (10^{-4})	42	6.32	92	6.66	83	6.62
		46	6.36	81	6.61	62	6.49
		47	6.37	67	6.52	65	6.51
	STDEV		0.02645751		0.070946		0.07
	Average		6.35		6.59		6.54
VSV-S	12 h (10^{-4})	56	6.44	36	6.25	7 (10^{-4})	5.54
		47	6.37	39	6.29	5 (10^{-4})	5.39
		46	6.63	25	6.09	42 (10^{-3})	5.32
	STDEV		0.13453624		0.10583		0.112398
	Average		6.48		6.21		5.41
VSV-MCP	12 h (10^{-3})	65	5.51	14	4.84	27 (10^{-2})	4.13
		67	5.52	11	4.74	22 (10^{-2})	4.04
		61	5.48	9	4.65	15 (10^{-2})	3.87
	STDEV		0.02081666		0.095044		0.132035
	Average		5.5		4.74		4.01
VSV-S	8 h	18 (10^{-4})	5.95	13 (10^{-3})	4.81	14 (10^{-2})	3.84
		23 (10^{-4})	6.06	14 (10^{-3})	4.84	25 (10^{-2})	4.09
		27 (10^{-4})	6.13	16 (10^{-3})	4.9	31 (10^{-2})	4.19
	STDEV		0.09073772		0.045826		0.180278
	Average		6.04		4.85		4.04

Virus	POST INFECTION (h)	MOI=1		MOI=0.1		MOI=0.01	
		# of plaques	PFU/ml (log 10)	# of plaques	PFU/ml (log 10)	# of plaques	PFU/ml (log 10)
VSV-MCP	8 h	45 (10^{-2})	4.35	27 (10^{-1})	3.13	6 (10^{-1})	2.47
		52 (10^{-2})	4.41	30 (10^{-1})	3.17	8 (10^{-1})	2.6
		47 (10^{-2})	4.37	39 (10^{-1})	3.29	10 (10^{-1})	2.69
	STDEV		0.0305505		0.083267		0.110604
	Average		4.37		3.19		2.58
VSV-S	4 h	41	3.31	0	0	0	0
		43	3.33	0	0	0	0
		38	3.28	0	0	0	0
	STDEV		0.02516611		0		0
	Average		3.3				
VSV-MCP	4 h	0	0	0	0	0	0
		0	0	0	0	0	0
		0	0	0	0	0	0
	Average	0	0	0	0	0	0

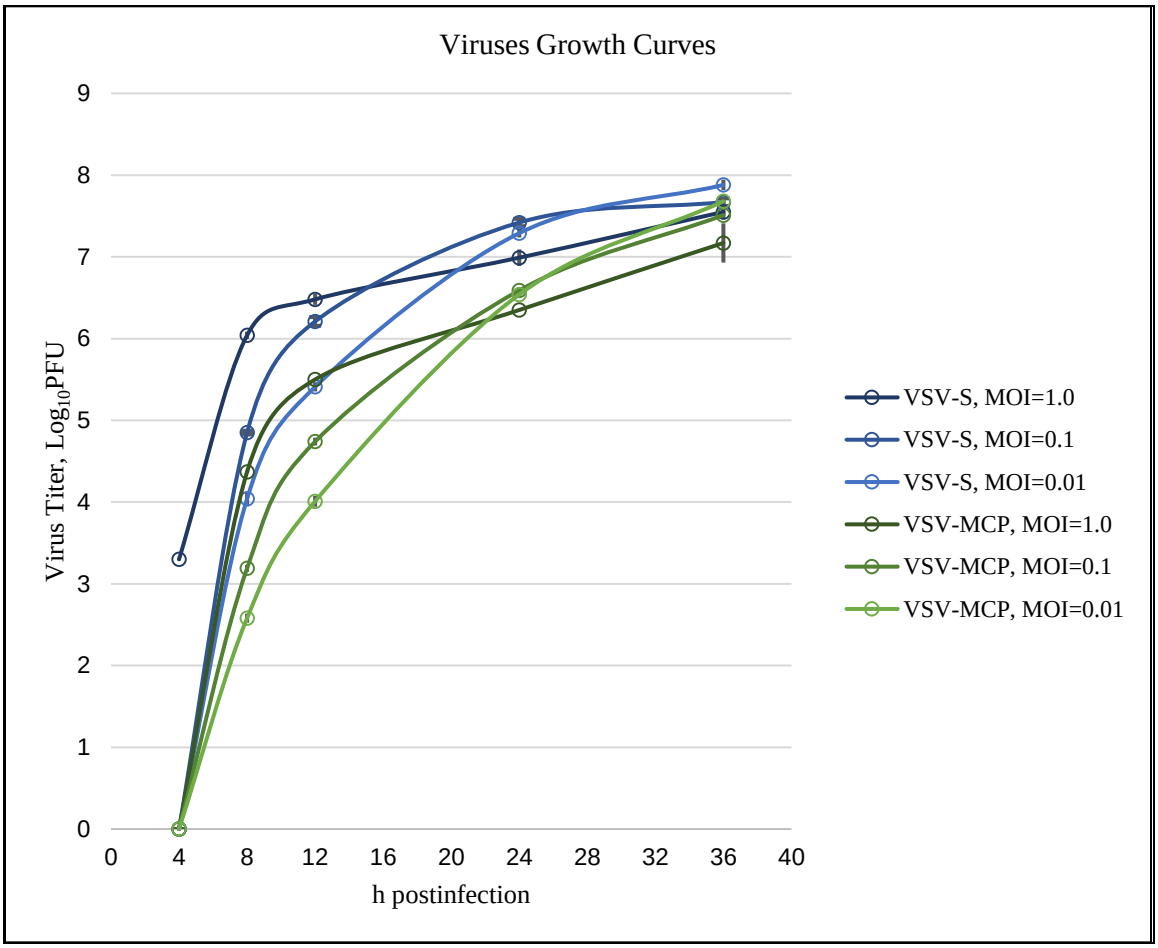

Figure 5. Growth curves of VSV-MCP and VSV-S. Supernatants from infected HeLa cells (MOI=0.01, 0.1, 1) were collected at 4, 8, 12, 24 and 36 h post infection and titers were measured by plaque assay.

3.2 Virus purification

For studies of antitumor activities in animal models, viruses were purified and concentrated. Supernatants from infected HeLa cells (MOI=0.1) were collected and viruses were purified following steps of the purification protocol described at section 2.5. The titers of the purified VSV-S and VSV-MCP were examined by plaque assay (Fig. 6. and Table (4)). The results showed VSV-S grew at the same and/or higher titer as VSV-MCP.

Viruses were also propagated in Vero cells. Supernatants of infected Vero cells (MOI=0.1) were collected and viruses were purified following steps of the purification protocol described at section 2.5. The titers were determined by plaque assay. The similar pattern of growth was observed for VSV-S and VSV-MCP infection of HeLa cells (Fig. 7).

All of these data indicating that armed VSV has the similar or higher titer compare to VSV-MCP and we conclude that insertion and expression of Smac does not comprise VSV replication.

Table (4). Titer of purified VSV-MCP and VSV-S, using HeLa cells

Virus	$Log_{10}PFU$						
VSV-MCP	6.87	7.65	7.74	8.95	7.93	7.97	8.54
VSV-S	8.6	8.39	8.47	9.04	7.87	8.38	8.65

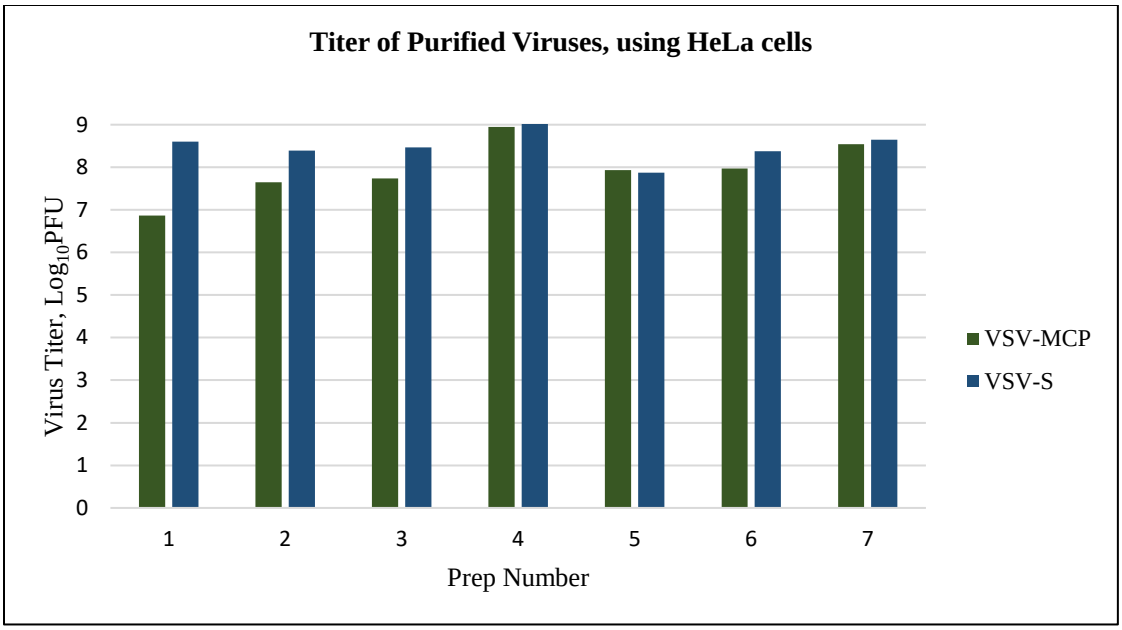

Figure 6. Titers of purified VSV-S and VSV-MCP. Different purified samples were from infected HeLa cells (MOI=0.1) and titers were measured by plaque assay.

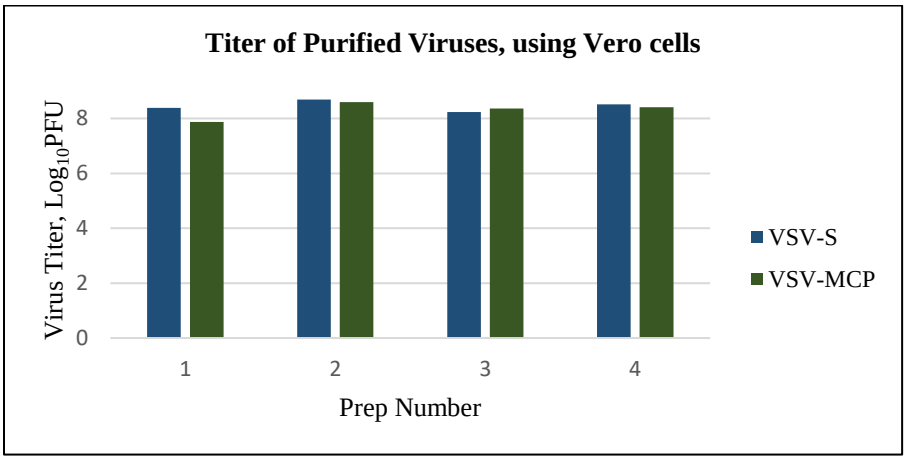

Figure 7. Titers of purified VSV-MCP and VSV-S. Different purified samples were from infected Vero cells (MOI=0.1) and titers were measured by plaque assay.

3.3 VSV-S enhanced apoptosis

Evidence from different literature showed that apoptosis pathway was triggered after VSV infection through intrinsic or mitochondrial pathway (78, 84, 85). Several studies also confirmed that overexpression of Smac or applying Smac mimetic compounds could directly trigger cancer cell death or sensitized tumor cells to other cancer therapeutic agents (80, 81, 87, 89, 90). We wanted to investigate the enhancement of apoptosis through overexpression of Smac upon infection by VSV-S, compared to VSV-MCP as a control. In order to evaluate apoptosis, expression level of Smac, cleaved caspase 3 and 9 (key proteins involved in intrinsic apoptosis pathway) were analyzed in HeLa cells following infection by VSV-S and VSV-MCP via western blot. HeLa cells were grown in DMEM supplemented with 10% FBS and 1% penicillin/streptomycin and seeded in 100 mm plates. After removing the old media, cells were washed with warm DPBS and infected with VSV-S and VSV-MCP, respectively. At different time points (0, 12 and 24 h post infection), cells were washed by ice-cold PBS and lysed by RIPA lysis buffer. Following steps described at section 2.7 and using Smac, cleaved caspase 3 and 9 antibodies, the level of these proteins was monitored (Fig. 8 and 9). The antibody used for detecting Smac could detect full length (27 kDa) and mature form (21 kDa) of Smac.

The data in Fig. 8 showed a significant increase in the level of Smac expression following infection of VSV-S. Since Smac (full length) was expressed by VSV-S during virus infection, this increasing level was expected. Full length Smac expressed by VSV-S was processed to form the mature Smac (Δ55 Smac). There was an increase in the level of mature Smac, but the majority of Smac protein expressed by VSV-S was full length, which means Smac expression by VSV-S did not result in premature release of Δ55 Smac so the virus could continue to be produced before activation of apoptosis in the infected cell. At 24 h post infection, although the large portion of

cells had died as indicated by the reduced level of GAPDH, the level of Smac expression was still high. On the other hand, the level of mature Smac was reduced at 12 h post infection and its level became hard to detect at 24 h post infection, upon infection of VSV-MCP. The rate of cell death was also lower for cells infected by VSV-MCP compared to VSV-S, as indicated by the level of GAPDH. One way for VSV to deplete mature Smac is by inducing mitophagy because mature Smac resides in the intermembrane space of mitochondria. Another potential mechanism of Smac removal is by Smac ubiquitination activated by wt VSV infection (91).

The results in Fig. 9 showed an increase in the level of cleaved caspase 3 after 24 hour post infection by VSV-S. For VSV-MCP the bands were almost undetectable, which is consistence with previous result confirming that intrinsic apoptosis pathway was not activated by VSV-MCP. Unfortunately, we could not detect the level of cleaved caspase 9 to better evaluate apoptosis by this experiment.

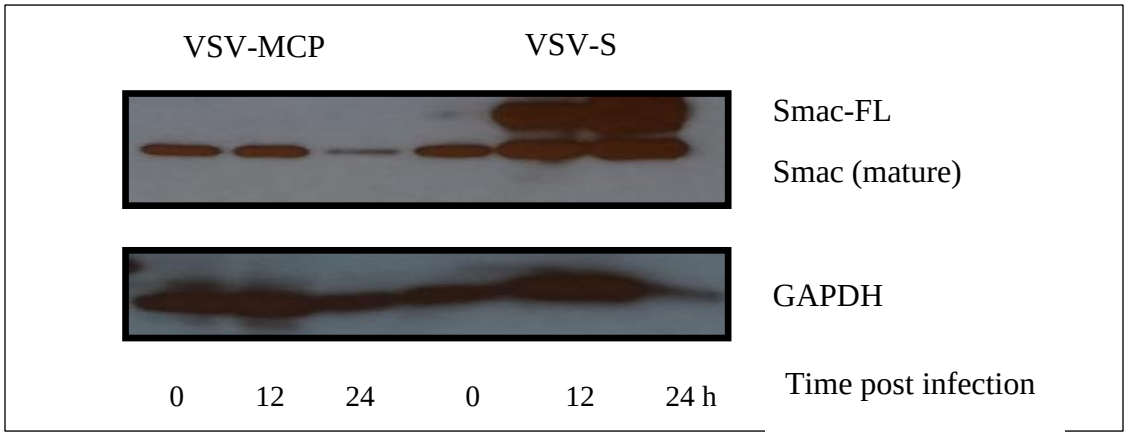

Figure 8. Level of Smac (full length and mature) in response to VSV-MCP and VSV-S infection. HeLa cells were infected by viruses and lysed at 0, 12 and 24 hour post infection and subjected to western blot analysis. GAPDH was used as a loading control.

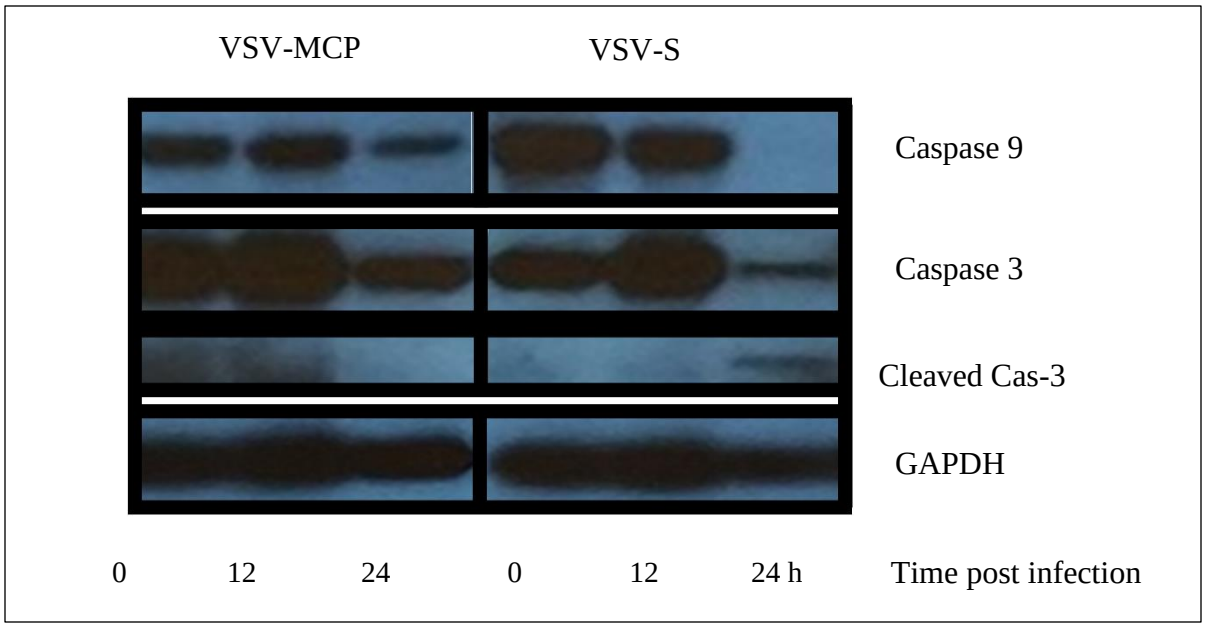

Figure 9. Evaluating levels of caspase 3 and 9 by western blot. HeLa cells were infected by VSV-S and VSV-MCP. GAPDH was used as a loading control.

3.4 Assessing autophagy progression

Many studies showed that some viruses (such as NDV, VSV) take advantage of autophagy to enhance viral replication and release (79, 92-97). It has been shown that NDV, which is in the same virus class as VSV, induces autophagy. The level of LC3 II was increased in A549 cells following infection by NDV (79). Based on these studies, autophagy appears to play a cytoprotective role against apoptosis in infected cells.

Here we studied autophagy activation after VSV-MCP and VSV-S infection, by using HeLa cell lines expressing GFP-LC3 (98) through monitoring GFP-LC3 puncta.

HeLa cells expressing GFP-LC3 were cultured in DMEM supplemented with 10% FBS and 1% penicillin/streptomycin and seeded in 6-well plates with glass coverslip at the bottom. As a positive control, rapamycin (2 μM), a well-known autophagy inducer by suppressing mTOR,

was used. Chloroquine (40 μM), an inhibitor of autophagic degradation in the lysosomes, was added to all media. 40 μM is the minimal saturating concentration of chloroquine necessary to reach maximal suppression of autophagy in HeLa cells (98). After removing old media, cells were washed with warm DPBS, and infected with VSV-S and VSV-MCP, respectively, at MOI=10. The cells that were not infected and treated with rapamycin, considered as a positive control. At different time points (0, 2, 6, 10 and 24 h post infection), coverslips were washed with DPBS, and cells were fixed by formaldehyde (10%) for 15 min. Following steps as described in section 2.9, slides were prepared and images were taken under a fluorescent microscope. The number of GFP-LC3 puncta was counted for 15 cells under each different condition (Fig. 10).

The result showed VSV-MCP induced autophagy during infection, which was monitored by appearance of GFP-LC3 puncta after 6 h post infection. After 10 h, there were few cells left on coverslips and they had the same morphology as the control cells, which indicated that they were not actually infected. For cells infected with VSV-S, the remaining cells on the coverslips were much fewer. These results suggest that autophagy may promote viral replication and mainly plays a cytoprotective role in infected cells.

To further confirm the role of autophagy in VSV infection, the conversion of LC3-I to LC3-II was analyzed by western blot. In order to assess the level of LC3-I and LC3-II , HeLa cells were were seeded into 6-well plates and infected with VSV-MCP and VSV-S, respectively, at MOI=1.0 for 0, 12 and 24 hours. The expression level of LC3-I and LC3-II was analyzed via western blot analysis described in section 2.7 , using LC3 antibody that was able to recognize LC3-I at molecular weight around 16 kDa and LC3-II at 18 kDa, respectively, (Fig. 11). The results showed after 24 h post infection, LC3-II was depleted for both VSV-MCP and VSV-S and the

ratio of LC3-II/LC3-I did not seem to change much. However, this experiment needs to be repeated because the cells may not be in a very healthy state before starting the experiments.

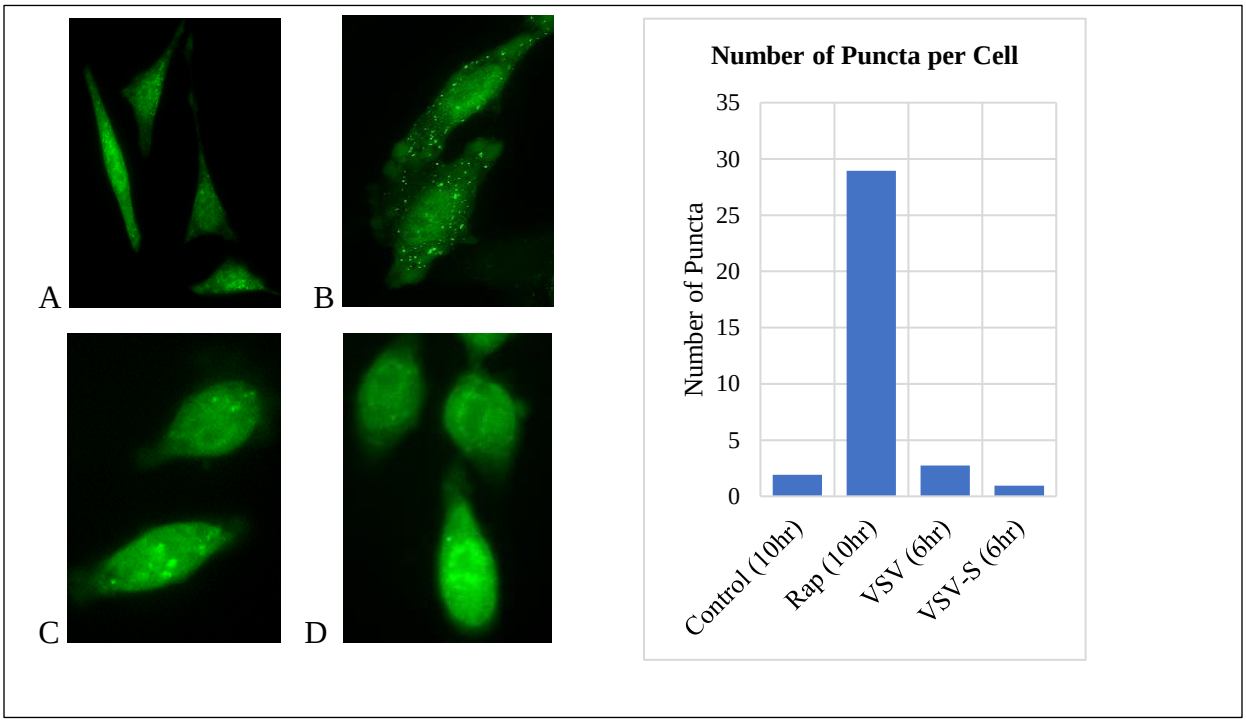

Figure 10. Puncta of LC3. (A) HeLa GFP-LC3 as a control, (B) rapamycin (2 µM) as a positive control, after 10 h, (C) after 6 h of VSV-MCP infection and (D) after 6 h of VSV-S infection. Chloroquine (40 µM) was added to media. (E) Number of GFP-LC3 puncta per cell. 15 cells were counted under each condition.

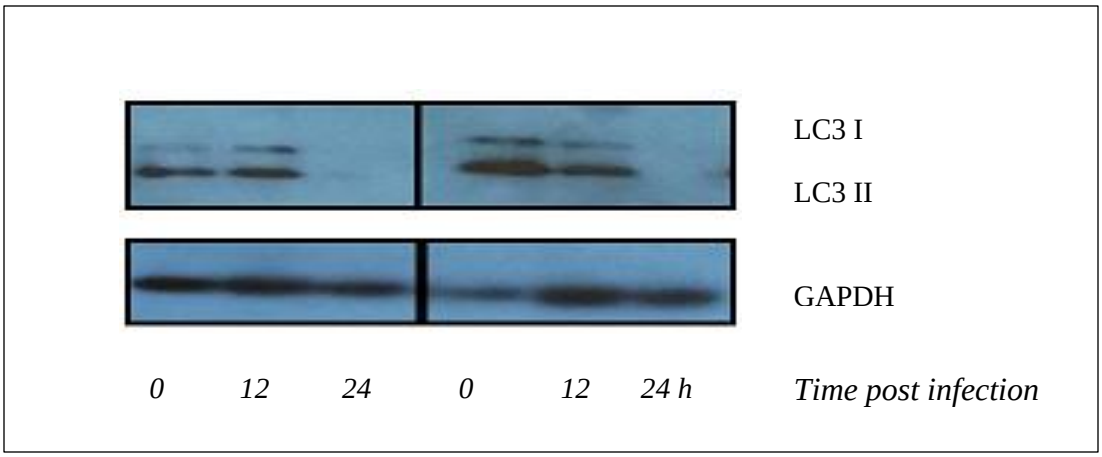

Figure 11. Levels of LC3 I and LC3 II. HeLa cells were infected by VSV-MCP and VSV-S, respectively. Lysates were collected at 0, 12 and 24 h post infection and were analyzed by western blot with LC3 antibody.

3.5 In vitro efficacy of cancer cell killing by VSV-MCP, VSV-S and VSV-Δ55S

In order to evaluate the potential of cancer cell killing, T-47D breast cancer cells were seeded in 12-well plates and infected with VSV-MCP, VSV-S and VSV-Δ55S, respectively, at MOI=5. Cell viability was measured at 24 and 48 h post infection by MTT assay. The results (Fig. 12, Tables (5) and (6)) showed, after 24 and 48 h post infection, although all cells were infected by VSV-MCP but it could not effectively kill T-47D cells that have a high level of XIAP expression (99). After 24 h post infection, VSV-S and VSV- Δ55S were able to kill 30% and 35% of cells, respectively. The rate of cell death was also increased after 48 h post infection by armed viruses. VSV-S killed more than 75% of T-47D cells and VSV- Δ55S was able to kill 82% of T-47D cells.

We also measured the titer of collected supernatants at 24 and 48 h post infection by plaque assay. Fig. 13 and Table (7) represented the titer of armed viruses (VSV-S and VSV-Δ55S) compared to

VSV-MCP, which was consistence with results using HeLa cells. Interestingly at 24 h post infection, the titer of VSV-Δ55S was near 2 log higher, compared to VSV-S and VSV-MCP, but these differences reduced at 48 post infection, in the way that titer of VSV-S and VSV-Δ55S were closer but still one log higher than VSV-MCP. This may suggest that VSV-Δ55S induced apoptotic cell death sooner because no activation of Smac was needed, leading to a rapid spread of virus.

Table (5). Percentage of T-47D cell viability infected by VSV-MCP, VSV-S and VSV-Δ55S, at MOI=5, after 24 h post infection

Sample	Control	VSV-MCP	VSV-S	VSV-Δ55S	Triton 1%
Absorbance	1.492	1.629	1.225	1.134	0.337
	1.715	1.668	1.124	1.248	0.287
	-----	------	1.351	1.075	------
% cell viability	100%	100%	71%	65%	-------

Table (6). Percentage of T-47D cell viability infected by VSV-S and VSV-Δ55S, at MOI=5, after 48 h post infection

Sample	Control	VSV-S	VSV-Δ55S	Triton 1%
Absorbance	1.306	0.390	0.410	0.153
	1.783	0.665	0.503	0.223
	1.468	0.565	0.491	0.246
% cell viability	100%	25.36%	19.88%	--------

A

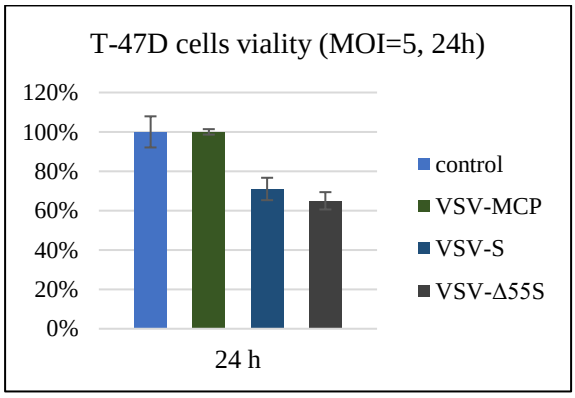

B

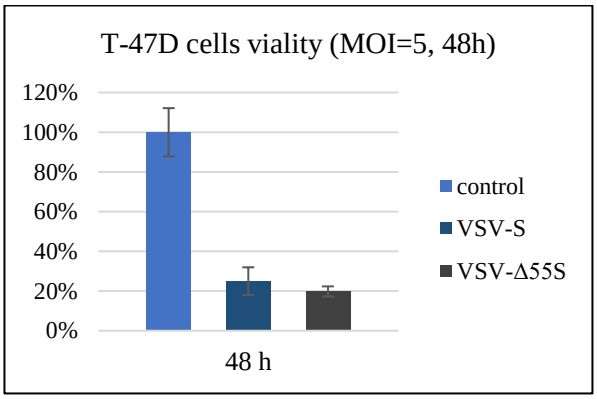

Figure 12. In vitro efficacy of VSV-S and VSV-Δ55S. (A) After 24 post infection, VSV-MCP could not kill T-47D cells effectively, but more than 35% of cells were dead by infection of armed viruses. (B) The rate of cell death increased significantly at 48 h post infection by VSV-S and VSV-Δ55S.

Table (7). Titer of armed viruses and VSV-MCP (MOI=5) at 24 and 48 h post infection, using T-47D cells.

Viruses	**VSV-MCP**		**VSV-S**		**VSV-Δ55S**	
Time point	24h	48h	24h	48h	24h	48h
Titer of virus (Log_{10}PFU)	5.3	5.54	5.3	7	7.17	7.87
	5.17	6.69	5.47	7.3	7.4	7.54
	-------	-------	5.6	7.17	7.49	7.9
Average	5.235	6.115	5.456667	7.156667	7.353333	7.77
STDEV	0.091924	0.813173	0.150444	0.150444	0.165025	0.19975

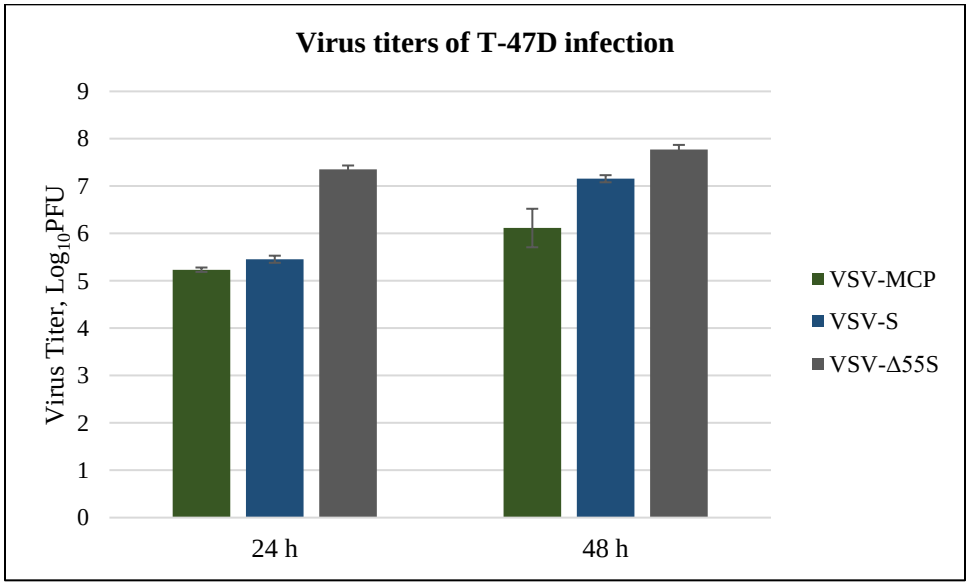

Figure 13. Virus titers from T-47D cells infected by different viruses (MOI=5). Supernatants of infected T-47D cells were collected at 24 and 48 h post infection and titers were measured by plaque assay.

3.6 ex vivo infection of carcinoma canine oral and anal carcinoma tissues

We also confirmed the ability of VSV-MCP and VSV-S in ex vivo infection of carcinoma canine oral and carcinoma anal tissues. Even cuts from different regions of the tissues were placed in 12-well plate and washed three times with warm DPBS. 1×10^{5} PFU of viruses was added to each well and after one hour of virus absorption, the virus inoculum was removed and fresh media were added. Supernatants of infected tissues were collected at 72 h post infection and titers were measured by plaque assay. The titer of viruses confirmed the ability of viruses to infect and replicate in canine carcinoma tissues (Fig. 14).

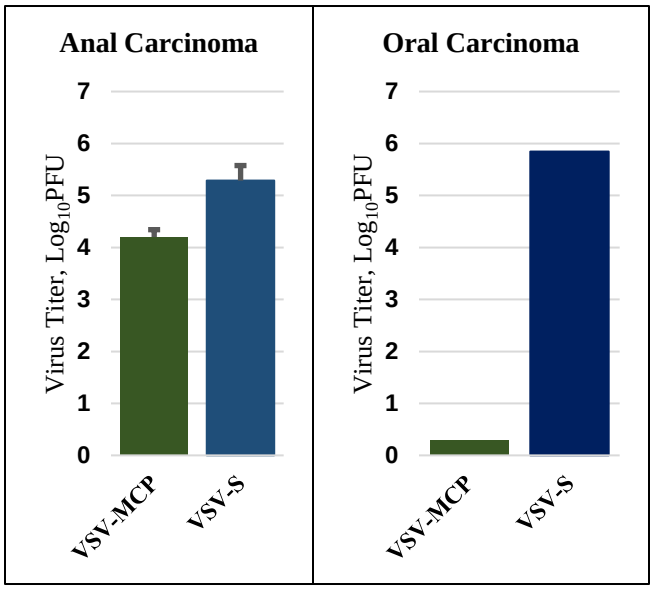

Figure. 14. ex vivo infection of canine carcinoma tissues with VSV-S and VSV-MCP, respectively. Supernatants from canine anal and oral carcinoma tissues infected with VSV-S and VSV-MCP, respectively, were collected at 72 h post infection and titers were measured by plaque assay.

CHAPTER 4: CONCLUSIONS

Oncolytic virotherapy has caught a lot of many attention and is becoming one of the promising methods to treat cancer (100). Applying virus will cause a direct oncolytic effect on the tumor because of its replication and also will trigger the host immune response to viral particles, tumor associated antigens and other proteins. The viruses need to have specific characteristics in order to be appropriate for virotherapy. The safety aspect of administrating viruses must be considered carefully, in the other words; they should be able to target cancerous cells and having no harmful effects on healthy tissues. Advancement in genetic engineering made it possible for researchers to design recombinant viruses, which were more specific, and having better oncolytic effects (101, 102).

VSV has many prerequisites of a better oncolytic vector and different kinds of modification have been done on its genome to enhance the efficacy of VSV to destroy malignant cells (12). Previous studies showed that some viruses like VSV, NDV and many other viruses manipulate the autophagy pathway to enhance their replication and survival. However, the exact mechanism on how viruses take advantages of autophagy for their replication is still unclear in most cases and it depends on cell types, virus strains or serotypes (12, 18). It also has been shown that, VSV infection induces apoptosis through the intrinsic mitochondrial pathway (78, 84, 103) and inhibition of autophagy enhances induction of apoptosis by VSV (95). Autophagy promotes viral replication and plays a cytoprotective role in cancer cells by inhibiting apoptosis, so it should be blocked by administrating autophagy inhibitor at later stage in order to trigger apoptosis and having more profound oncolytic effects (79). Therefore, for having the best oncolytic effect, it is necessary to inhibit autophagy after sufficient virus replication. We have designed two engineered

viruses by inserting a suicide gene (Smac) in its full length (VSV-S) and mature form (VSV-Δ55S) between the M and G genes of VSV genome to achieve this goal.

During induction of intrinsic apoptosis pathway, the mature form of Smac, originated by the cleavage of 55 N-terminus amino acids that serve as mitochondrial targeting signal (MTS), is released to cytosol. The mature form of Smac interacts with IAPs (inhibitory proteins of apoptosis) in the cytosol, which results in the activation of caspases and apoptosis. The four hydrophobic amino acids, Ala-Val-Pro-Ile, at the N-terminus of Smac are responsible for interacting with the BIR2 and BIR3 domains of XIAP, resulting in the release of caspase-3 and caspase 9, respectively (80, 81). Several studies showed that overexpression of Smac sensitized tumor cells to apoptotic death. Therefore, engineering VSV by insertion of Smac should result in more apoptotic activities of this virus.

Here we performed several experiments to evaluate and compare the oncolytic effects of wild type VSV expressing mCherry fused P protein (VSV-MCP) as a control and armed VSV-S and VSV-Δ55S.

The first thing to examine was the effect of Smac insertion on virus replication. Since VSV genome is a negative sense single RNA strand, it serves as a template to synthesize five messenger RNAs in a decreasing order of molar ratios as N>P>M>G>L which are then translated by host ribosomes to produce viral proteins. The abundance of these proteins is related to location of coding region from the 3′ end of the genome (104, 105). N, P and M proteins are essential for viral assembly and replication, and therefore insertion of Smac between M and G genes should not have any impact on armed VSV replication. Beside this, the level of Smac is also related to replication of the armed VSV, which will not limit the replication cycle due to the delay of expression (based on the obligatorily sequential of transcription of VSV genome).

Based on the results of virus growth curve at different MOI, and titers of viruses using several cell lines, the growth rate of engineered VSV was the same or higher compared to VSV-MCP as a control, confirming that insertion of Smac does not comprise virus replication.

Our results also indicate that the rate of cell death increased upon infection by VSV-S or VSV-Δ55S compare to VSV-MCP as a control. At 24 h post-infection VSV-MCP was not able to effectively kill T-47D cells which have a high level of XIAP expression, but the percentage of cell death were more than 35% by infection of VSV-S or VSV-Δ55S. The results also showed a significant increase in cell death after 48 h post infection by armed viruses, which suggests that these newly engineered viruses have a higher efficacy in killing cancerous cells compared to wild type VSV.

We also investigated autophagy progression, by monitoring GFP-LC3 puncta at different time points if infection by VSV-MCP or VSV-S using HeLa cells expressing GFP-LC3 . Rapamycin (2 μM) was used as a positive control. The results showed appearance of puncta after 6 h post infection, indicating autophagy induction by VSV-MCP. After 10 and 24 h, few cells were left having the same morphology as the control cells, suggesting they were not infected. For VSV-S the rate of cell death was higher and it was difficult to find cells that were still present on the coverslip. These data confirmed that autophagy induction by VSV mainly plays a cytoprotective role and there was suppression of autophagy by VSV-S. However, more studies should be done in order to evaluate autophagy progression by monitoring autophagy flux and the exact mechanism on how VSV induces autophagy and inhibits apoptosis.

Another piece of evidence confirming induction of apoptosis following VSV-S infection was assessing levels of Smac, cleaved caspase-3 and 9, which are the key proteins in regulating apoptosis pathway. Western blot analysis of lysed HeLa cells infected by VSV-S and VSV-MCP,

respectively, at 0, 12 and 24 h post infection, showed an increase in the level of Smac (mature form) in VSV-S infected cells, indicating apoptosis induction and higher rate of cell death by VSV-S comparde to VSV-MCP. There was also an increase in the level of cleaved caspase 3 after 24 h post infection by VSV-S. Unfortunately we couldn't detect the level of cleaved caspase 9 for this experiment.

In conclusion, our results showed armed VSV by inserting Smac expressing unit in VSV genome does not comprise viral replication and this enhanced the efficacy of armed viruses in killing cancerous cells. Further investigation should be carried out to demonstrate how VSV induced autophagy to inhibit apoptosis and to determine the mechanism of apoptosis induction by VSV-S.

REFERENCES

1. Howells A, Marelli G, Lemoine NR, Wang Y. Oncolytic Viruses—Interaction of Virus and Tumor Cells in the Battle to Eliminate Cancer. Frontiers in Oncology. 2017;7(195).

2. Pack GT. Note on the experimental use of rabies vaccine for melanomatosis. AMA archives of dermatology and syphilology. 1950;62(5):694-5.
3. Everts B, van der Poel HG. Replication-selective oncolytic viruses in the treatment of cancer. Cancer Gene Therapy. 2004;12:141.
4. Vähä-Koskela MJV, Heikkilä JE, Hinkkanen AE. Oncolytic viruses in cancer therapy. Cancer Letters. 2007;254(2):178-216.
5. Kelly E, Russell SJ. History of Oncolytic Viruses: Genesis to Genetic Engineering. Molecular Therapy. 2007;15(4):651-9.
6. Fukuhara H, Ino Y, Todo T. Oncolytic virus therapy: A new era of cancer treatment at dawn. Cancer Science. 2016;107(10):1373-9.
7. Kaufman HL, Kohlhapp FJ, Zloza A. Oncolytic viruses: a new class of immunotherapy drugs. Nature Reviews Drug Discovery. 2015;14:642.
8. Choi AH, O'Leary MP, Fong Y, Chen NG. From Benchtop to Bedside: A Review of Oncolytic Virotherapy. Biomedicines. 2016;4(3):18.
9. Chiocca EA, Rabkin SD. Oncolytic Viruses and Their Application to Cancer Immunotherapy. Cancer immunology research. 2014;2(4):295-300.
10. Zeyaullah M, Patro M, Ahmad I, Ibraheem K, Sultan PS, Nehal M, et al. Oncolytic Viruses in the Treatment of Cancer: A Review of Current Strategies2012. 771-81 p.
11. Filley AC, Dey M. Immune System, Friend or Foe of Oncolytic Virotherapy? Front Oncol. 2017;7:106.
12. Balachandran S, Barber GN. Vesicular Stomatitis Virus (VSV) Therapy of Tumors. IUBMB Life. 2000;50(2):135-8.
13. Martinez I, Wertz GW. Biological Differences between Vesicular Stomatitis Virus Indiana and New Jersey Serotype Glycoproteins: Identification of Amino Acid Residues Modulating pH-Dependent Infectivity. Journal of virology. 2005;79(6):3578-85.
14. Bishnoi S, Tiwari R, Gupta S, Byrareddy S, Nayak D. Oncotargeting by Vesicular Stomatitis Virus (VSV): Advances in Cancer Therapy. Viruses. 2018;10(2):90.
15. Zhang JLaY. Messenger RNA Cap Methylation in Vesicular Stomatitis Virus, a Prototype of Non-Segmented Negative-Sense RNA Virus, Methylation - From DNA, RNA and Histones to Diseases and Treatment, Prof. Anica Dricu (Ed.), InTech, . (2012).
16. Heiber JF, Xu X-X, Barber GN. Potential of vesicular stomatitis virus as an oncolytic therapy for recurrent and drug-resistant ovarian cancer. Chinese Journal of Cancer. 2011;30(12):805-14.
17. Green TJ, Luo M. Structure of the vesicular stomatitis virus nucleocapsid in complex with the nucleocapsid-binding domain of the small polymerase cofactor, P. Proceedings of the National Academy of Sciences. 2009;106(28):11713.
18. Harouaka D, Wertz GW. Mutations in the C-Terminal Loop of the Nucleocapsid Protein Affect Vesicular Stomatitis Virus RNA Replication and Transcription Differentially. Journal of virology. 2009;83(22):11429-39.

19. Nayak D, Panda D, Das SC, Luo M, Pattnaik AK. Single-Amino-Acid Alterations in a Highly Conserved Central Region of Vesicular Stomatitis Virus N Protein Differentially Affect the Viral Nucleocapsid Template Functions. Journal of virology. 2009;83(11):5525-34.
20. Li J, Zhang Y. Messenger RNA Cap Methylation in Vesicular Stomatitis Virus, a Prototype of Non-Segmented Negative-Sense RNA Virus2012. 237-70 p.
21. Emerson SU, Yu Y. Both NS and L proteins are required for in vitro RNA synthesis by vesicular stomatitis virus. Journal of virology. 1975;15(6):1348-56.
22. Masters PS, Banerjee AK. Complex formation with vesicular stomatitis virus phosphoprotein NS prevents binding of nucleocapsid protein N to nonspecific RNA. Journal of virology. 1988;62(8):2658-64.
23. Emerson SU, Yu Y. Both NS and L proteins are required for in vitro RNA synthesis by vesicular stomatitis virus. Journal of virology. 1975;15(6):1348-56.
24. Ogino T, Banerjee AK. Unconventional mechanism of mRNA capping by the RNA-dependent RNA polymerase of vesicular stomatitis virus. Molecular cell. 2007;25(1):85-97.
25. Swinteck BD, Lyles DS. Plasma Membrane Microdomains Containing Vesicular Stomatitis Virus M Protein Are Separate from Microdomains Containing G Protein and Nucleocapsids. Journal of virology. 2008;82(11):5536-47.
26. Jayakar HR, Whitt MA. Identification of Two Additional Translation Products from the Matrix (M) Gene That Contribute to Vesicular Stomatitis Virus Cytopathology. Journal of virology. 2002;76(16):8011-8.
27. Chong LD, Rose JK. Interactions of normal and mutant vesicular stomatitis virus matrix proteins with the plasma membrane and nucleocapsids. Journal of virology. 1994;68(1):441-7.
28. Lenard J, Vanderoef R. Localization of the membrane-associated region of vesicular stomatitis virus M protein at the N terminus, using the hydrophobic, photoreactive probe 125I-TID. Journal of virology. 1990;64(7):3486-91.
29. Ahmed M, McKenzie MO, Puckett S, Hojnacki M, Poliquin L, Lyles DS. Ability of the matrix protein of vesicular stomatitis virus to suppress beta interferon gene expression is genetically correlated with the inhibition of host RNA and protein synthesis. Journal of virology. 2003;77(8):4646-57.
30. Kopecky SA, Lyles DS. The Cell-Rounding Activity of the Vesicular Stomatitis Virus Matrix Protein Is due to the Induction of Cell Death. Journal of virology. 2003;77(9):5524-8.
31. Enninga J, Levy DE, Blobel G, Fontoura BM. Role of nucleoporin induction in releasing an mRNA nuclear export block. Science. 2002;295(5559):1523-5.
32. Balachandran S, Roberts PC, Kipperman T, Bhalla KN, Compans RW, Archer DR, et al. Alpha/beta interferons potentiate virus-induced apoptosis through activation of the FADD/Caspase-8 death signaling pathway. Journal of virology. 2000;74(3):1513-23.
33. Lichty BD, Power AT, Stojdl DF, Bell JC. Vesicular stomatitis virus: re-inventing the bullet. Trends Mol Med. 2004;10(5):210-6.
34. Sinkovics JG, Horvath J. Can virus therapy of human cancer be improved by apoptosis induction? Medical Hypotheses. 1995;44(5):359-68.
35. Carneiro FA, Bianconi ML, Weissmüller G, Stauffer F, Da Poian AT. Membrane Recognition by Vesicular Stomatitis Virus Involves Enthalpy-Driven Protein-Lipid Interactions. Journal of virology. 2002;76(8):3756-64.
36. Puri A, Winick J, Lowy RJ, Covell D, Eidelman O, Walter A, et al. Activation of vesicular stomatitis virus fusion with cells by pretreatment at low pH. The Journal of biological chemistry. 1988;263(10):4749-53.

37. Publicover J, Ramsburg E, Rose JK. A Single-Cycle Vaccine Vector Based on Vesicular Stomatitis Virus Can Induce Immune Responses Comparable to Those Generated by a Replication-Competent Vector. Journal of virology. 2005;79(21):13231-8.
38. Finkelshtein D, Werman A, Novick D, Barak S, Rubinstein M. LDL receptor and its family members serve as the cellular receptors for vesicular stomatitis virus. Proceedings of the National Academy of Sciences of the United States of America. 2013;110(18):7306-11.
39. Schlegel R, Tralka TS, Willingham MC, Pastan I. Inhibition of VSV binding and infectivity by phosphatidylserine: is phosphatidylserine a VSV-binding site? Cell. 1983;32(2):639-46.
40. Matlin KS, Reggio H, Helenius A, Simons K. Pathway of vesicular stomatitis virus entry leading to infection. Journal of molecular biology. 1982;156(3):609-31.
41. Cureton DK, Massol RH, Saffarian S, Kirchhausen TL, Whelan SP. Vesicular stomatitis virus enters cells through vesicles incompletely coated with clathrin that depend upon actin for internalization. PLoS pathogens. 2009;5(4):e1000394.
42. Follett EAC, Pringle CR, Wunner WH, Skehel JJ. Virus Replication in Enucleate Cells: Vesicular Stomatitis Virus and Influenza Virus. Journal of virology. 1974;13(2):394-9.
43. Barr JN, Tang X, Hinzman E, Shen R, Wertz GW. The VSV polymerase can initiate at mRNA start sites located either up or downstream of a transcription termination signal but size of the intervening intergenic region affects efficiency of initiation. Virology. 2008;374(2):361-70.
44. Barr JN, Whelan SP, Wertz GW. Transcriptional control of the RNA-dependent RNA polymerase of vesicular stomatitis virus. Biochimica et biophysica acta. 2002;1577(2):337-53.
45. Rowlands DJ. Sequences of vesicular stomatitis virus RNA in the region coding for leader RNA, N protein mRNA, and their junction. Proceedings of the National Academy of Sciences of the United States of America. 1979;76(10):4793-7.
46. Peluso RW. Kinetic, quantitative, and functional analysis of multiple forms of the vesicular stomatitis virus nucleocapsid protein in infected cells. Journal of virology. 1988;62(8):2799-807.
47. Whitlow ZW, Connor JH, Lyles DS. Preferential translation of vesicular stomatitis virus mRNAs is conferred by transcription from the viral genome. Journal of virology. 2006;80(23):11733-42.
48. Mebatsion T, Weiland F, Conzelmann KK. Matrix protein of rabies virus is responsible for the assembly and budding of bullet-shaped particles and interacts with the transmembrane spike glycoprotein G. Journal of virology. 1999;73(1):242-50.
49. Robison CS, Whitt MA. The Membrane-Proximal Stem Region of Vesicular Stomatitis Virus G Protein Confers Efficient Virus Assembly. Journal of virology. 2000;74(5):2239-46.
50. Brown EL, Lyles DS. Organization of the Vesicular Stomatitis Virus Glycoprotein into Membrane Microdomains Occurs Independently of Intracellular Viral Components. Journal of virology. 2003;77(7):3985-92.
51. Das SC, Nayak D, Zhou Y, Pattnaik AK. Visualization of Intracellular Transport of Vesicular Stomatitis Virus Nucleocapsids in Living Cells. Journal of virology. 2006;80(13):6368-77.
52. Das SC, Nayak D, Zhou Y, Pattnaik AK. Visualization of intracellular transport of vesicular stomatitis virus nucleocapsids in living cells. Journal of virology. 2006;80(13):6368-77.
53. Harty RN, Paragas J, Sudol M, Palese P. A proline-rich motif within the matrix protein of vesicular stomatitis virus and rabies virus interacts with WW domains of cellular proteins: implications for viral budding. Journal of virology. 1999;73(4):2921-9.
54. Strauss JH, Strauss EG. CHAPTER 4 - Minus-Strand RNA Viruses. Viruses and Human Disease (Second Edition). London: Academic Press; 2008. p. 137-91.

55. Heinrich BS, Cureton DK, Rahmeh AA, Whelan SP. Protein expression redirects vesicular stomatitis virus RNA synthesis to cytoplasmic inclusions. PLoS pathogens. 2010;6(6):e1000958.
56. Fernandez M, Porosnicu M, Markovic D, Barber GN. Genetically engineered vesicular stomatitis virus in gene therapy: application for treatment of malignant disease. Journal of virology. 2002;76(2):895-904.
57. Balachandran S, Porosnicu M, Barber GN. Oncolytic activity of vesicular stomatitis virus is effective against tumors exhibiting aberrant p53, Ras, or myc function and involves the induction of apoptosis. Journal of virology. 2001;75(7):3474-9.
58. Hastie E, Grdzelishvili VZ. Vesicular stomatitis virus as a flexible platform for oncolytic virotherapy against cancer. The Journal of General Virology. 2012;93(Pt 12):2529-45.
59. Rabinovich GA, Gabrilovich D, Sotomayor EM. Immunosuppressive strategies that are mediated by tumor cells. Annual review of immunology. 2007;25:267-96.
60. Critchley-Thorne RJ, Simons DL, Yan N, Miyahira AK, Dirbas FM, Johnson DL, et al. Impaired interferon signaling is a common immune defect in human cancer. Proc Natl Acad Sci U S A. 2009;106(22):9010-5.
61. Oliere S, Arguello M, Mesplede T, Tumilasci V, Nakhaei P, Stojdl D, et al. Vesicular Stomatitis Virus Oncolysis of T Lymphocytes Requires Cell Cycle Entry and Translation Initiation. Journal of virology. 2008;82(12):5735-49.
62. Platanias LC, Fish EN. Signaling pathways activated by interferons. Experimental hematology. 1999;27(11):1583-92.
63. Balachandran S, Barber GN. Defective translational control facilitates vesicular stomatitis virus oncolysis. Cancer Cell. 2004;5(1):51-65.
64. Barber GN. VSV-tumor selective replication and protein translation. Oncogene. 2005;24(52):7710-9.
65. Fernandez M, Porosnicu M, Markovic D, Barber GN. Genetically Engineered Vesicular Stomatitis Virus in Gene Therapy: Application for Treatment of Malignant Disease. Journal of virology. 2002;76(2):895-904.
66. Bi Z, Barna M, Komatsu T, Reiss CS. Vesicular stomatitis virus infection of the central nervous system activates both innate and acquired immunity. Journal of virology. 1995;69(10):6466-72.
67. Christian AY, Barna M, Bi Z, Reiss CS. Host immune response to vesicular stomatitis virus infection of the central nervous system in C57BL/6 mice. Viral immunology. 1996;9(3):195-205.
68. Zou W, Kim JH, Handidu A, Li X, Kim KI, Yan M, et al. Microarray analysis reveals that Type I interferon strongly increases the expression of immune-response related genes in Ubp43 (Usp18) deficient macrophages. Biochemical and biophysical research communications. 2007;356(1):193-9.
69. Hecht TT, Paul WE. Limitation of VSV infection by the host's response to VSV-associated cellular antigens. Journal of immunology (Baltimore, Md : 1950). 1982;129(4):1736-41.
70. Takaoka A, Yanai H. Interferon signalling network in innate defence. Cellular microbiology. 2006;8(6):907-22.
71. Burns JC, Friedmann T, Driever W, Burrascano M, Yee JK. Vesicular stomatitis virus G glycoprotein pseudotyped retroviral vectors: concentration to very high titer and efficient gene transfer into mammalian and nonmammalian cells. Proceedings of the National Academy of Sciences of the United States of America. 1993;90(17):8033-7.

72. Wollmann G, Rogulin V, Simon I, Rose JK, van den Pol AN. Some Attenuated Variants of Vesicular Stomatitis Virus Show Enhanced Oncolytic Activity against Human Glioblastoma Cells relative to Normal Brain Cells. Journal of virology. 2010;84(3):44-.
73. Nakhaei P, Paz S, Oliere S, Tumilasci V, Bell JC, Hiscott J. Oncolytic virotherapy of cancer with vesicular stomatitis virus. Gene Ther Mol Biol. 2005;9:269-80.
74. Barber GN. Vesicular stomatitis virus as an oncolytic vector. Viral immunology. 2004;17(4):516-27.
75. Wollmann G, Tattersall P, van den Pol AN. Targeting human glioblastoma cells: comparison of nine viruses with oncolytic potential. Journal of virology. 2005;79(10):6005-22.
76. Bischoff JR, Kirn DH, Williams A, Heise C, Horn S, Muna M, et al. An adenovirus mutant that replicates selectively in p53-deficient human tumor cells. Science. 1996;274(5286):373-6.
77. Melzer MK, Lopez-Martinez A, Altomonte J. Oncolytic Vesicular Stomatitis Virus as a Viro-Immunotherapy: Defeating Cancer with a "Hammer" and "Anvil". Biomedicines. 2017;5(1):8.
78. Pearce AF, Lyles DS. Vesicular Stomatitis Virus Induces Apoptosis Primarily through Bak Rather than Bax by Inactivating Mcl-1 and Bcl-XL. Journal of virology. 2009;83(18):9102-12.
79. Meng G, Xia M, Wang D, Chen A, Wang Y, Wang H, et al. Mitophagy promotes replication of oncolytic Newcastle disease virus by blocking intrinsic apoptosis in lung cancer cells. Oncotarget. 2014;5(15):6365-74.
80. Martinez-Ruiz G, Maldonado V, Ceballos-Cancino G, Grajeda JPR, Melendez-Zajgla J. Role of Smac/DIABLO in cancer progression. Journal of Experimental & Clinical Cancer Research : CR. 2008;27(1):48-.
81. Fandy TE, Shankar S, Srivastava RK. Smac/DIABLO enhances the therapeutic potential of chemotherapeutic drugs and irradiation, and sensitizes TRAIL-resistant breast cancer cells. Molecular cancer. 2008;7:60.
82. Mizushima N, Yoshimori T, Levine B. Methods in Mammalian Autophagy Research. Cell. 2010;140(3):313-26.
83. Gaddy DF, Lyles DS. Vesicular stomatitis viruses expressing wild-type or mutant M proteins activate apoptosis through distinct pathways. Journal of virology. 2005;79(7):4170-9.
84. Kopecky SA, Lyles DS. Contrasting effects of matrix protein on apoptosis in HeLa and BHK cells infected with vesicular stomatitis virus are due to inhibition of host gene expression. Journal of virology. 2003;77(8):4658-69.
85. Felt SA, Moerdyk-Schauwecker MJ, Grdzelishvili VZ. Induction of apoptosis in pancreatic cancer cells by vesicular stomatitis virus. Virology. 2015;474:163-73.
86. Cary ZD, Willingham MC, Lyles DS. Oncolytic Vesicular Stomatitis Virus Induces Apoptosis in U87 Glioblastoma Cells by a Type II Death Receptor Mechanism and Induces Cell Death and Tumor Clearance In Vivo. Journal of virology. 2011;85(12):5708-17.
87. Bai L, Smith DC, Wang S. Small-Molecule SMAC Mimetics as New Cancer Therapeutics. Pharmacology & therapeutics. 2014;144(1):82-95.
88. Dobson CC, Naing T, Beug ST, Faye MD, Chabot J, St-Jean M, et al. Oncolytic virus synergizes with Smac mimetic compounds to induce rhabdomyosarcoma cell death in a syngeneic murine model. Oncotarget. 2017;8(2):3495-508.
89. Fulda S. Promises and Challenges of Smac Mimetics as Cancer Therapeutics. Clinical cancer research : an official journal of the American Association for Cancer Research. 2015;21(22):5030-6.

90. Chen DJ, Huerta S. Smac mimetics as new cancer therapeutics. Anti-cancer drugs. 2009;20(8):646-58.
91. Hao Y, Sekine K, Kawabata A, Nakamura H, Ishioka T, Ohata H, et al. Apollon ubiquitinates SMAC and caspase-9, and has an essential cytoprotection function. Nature cell biology. 2004;6(9):849-60.
92. Espert L, Codogno P, Biard-Piechaczyk M. Involvement of autophagy in viral infections: antiviral function and subversion by viruses. Journal of molecular medicine (Berlin, Germany). 2007;85(8):811-23.
93. Chakrabarti A, Ghosh PK, Banerjee S, Gaughan C, Silverman RH. RNase L Triggers Autophagy in Response to Viral Infections. Journal of virology. 2012;86(20):11311-21.
94. Richetta C, Grégoire IP, Verlhac P, Azocar O, Baguet J, Flacher M, et al. Sustained Autophagy Contributes to Measles Virus Infectivity. PLOS Pathogens. 2013;9(9):e1003599.
95. Malilas W, Koh SS, Lee S, Srisuttee R, Cho IR, Moon J, et al. Suppression of autophagic genes sensitizes CUG2-overexpressing A549 human lung cancer cells to oncolytic vesicular stomatitis virus-induced apoptosis. Int J Oncol. 2014;44(4):1177-84.
96. Jounai N, Takeshita F, Kobiyama K, Sawano A, Miyawaki A, Xin KQ, et al. The Atg5 Atg12 conjugate associates with innate antiviral immune responses. Proc Natl Acad Sci U S A. 2007;104(35):14050-5.
97. Wang Y, Jiang K, Zhang Q, Meng S, Ding C. Autophagy in Negative-Strand RNA Virus Infection. Frontiers in Microbiology. 2018;9(206).
98. Ni HM, Bockus A, Wozniak AL, Jones K, Weinman S, Yin XM, et al. Dissecting the dynamic turnover of GFP-LC3 in the autolysosome. Autophagy. 2011;7(2):188-204.
99. Foster FM, Owens TW, Tanianis-Hughes J, Clarke RB, Brennan K, Bundred NJ, et al. Targeting inhibitor of apoptosis proteins in combination with ErbB antagonists in breast cancer. Breast Cancer Research : BCR. 2009;11(3):R41-R.
100. Sinkovics J, Horvath J. New developments in the virus therapy of cancer: a historical review. Intervirology. 1993;36(4):193-214.
101. Kirn DH, McCormick F. Replicating viruses as selective cancer therapeutics. Molecular Medicine Today. 1996;2(12):519-27.
102. Gromeier M. Oncolytic Viruses for Cancer Therapy. American Journal of Cancer. 2003;2(5):313-23.
103. Balachandran S, Roberts PC, Kipperman T, Bhalla KN, Compans RW, Archer DR, et al. Alpha/Beta Interferons Potentiate Virus-Induced Apoptosis through Activation of the FADD/Caspase-8 Death Signaling Pathway. Journal of virology. 2000;74(3):1513-23.
104. Ball LA, Pringle CR, Flanagan B, Perepelitsa VP, Wertz GW. Phenotypic Consequences of Rearranging the P, M, and G Genes of Vesicular Stomatitis Virus. Journal of virology. 1999;73(6):4705-12.
105. Wertz GW, Perepelitsa VP, Ball LA. Gene rearrangement attenuates expression and lethality of a nonsegmented negative strand RNA virus. Proceedings of the National Academy of Sciences of the United States of America. 1998;95(7):3501-6.